

Transmission Channel Analysis in Dynamic Models

July 12, 2024

Enrico Wegner^{2,*}, Lenard Lieb¹, Stephan Smeekes², and Ines Wilms²

¹*Department of Macro, International & Labour Economics, School of Business and Economics Maastricht*

²*Department of Quantitative Economics, School of Business and Economics Maastricht*

**Corresponding author: e.wegner@maastrichtuniversity.nl*

Abstract

We propose a framework for the analysis of transmission channels in a large class of dynamic models. To this end, we formulate our approach both using graph theory and potential outcomes, which we show to be equivalent. Our method, labelled Transmission Channel Analysis (TCA), allows for the decomposition of total effects captured by impulse response functions into the effects flowing along transmission channels, thereby providing a quantitative assessment of the strength of various transmission channels. We establish that this requires no additional identification assumptions beyond the identification of the structural shock whose effects the researcher wants to decompose. Additionally, we prove that impulse response functions are sufficient statistics for the computation of transmission effects. We demonstrate the empirical relevance of TCA for policy evaluation by decomposing the effects of policy shocks arising from a variety of popular macroeconomic models.

JEL CODES: C32, C54, E52, E60

KEYWORDS: transmission channel, policy evaluation, impulse response function, structural vector autoregression, DSGE, macroeconomic shocks

1 Introduction

In this paper we propose a formal framework for analysing transmission channels of causal effects that is applicable in a large family of dynamic models. Our framework allows to dynamically decompose the effects of interventions into a set of disjoint dynamic partial effects, where the choice of decomposition – the intervention’s transmission channel – is determined by the research question.

Our first contribution is the development of a formal framework that allows the study of precisely defined transmission channels. While there is an extensive literature in macroeconomics and time series econometrics on methodology for

studying the dynamic effects of interventions of shocks (see e.g. Kilian & Lütkepohl, 2017; Nakamura & Steinsson, 2018; Ramey, 2016b), the literature on formal analysis of transmission channels is relatively sparse. In macroeconomics, transmission channels are typically loosely defined as a collection of economic mechanisms that indirectly affect key macroeconomic outcomes through intermediate variables. However, a coherent quantitative framework for analysing transmission channels is missing. Instead, many studies analyse transmission channels qualitatively. From a policy perspective however, careful study of transmission channels is crucial. Given a particular total dynamic effect of the shock of interest, the relative importance of different transmission channels through which these total effects are realised can have major implications for designing effective policies. It is therefore crucial to have an unequivocal definition of transmission channels and accompanying methodology to decompose total effects accordingly.

Our second contribution is to formulate transmission channel analysis (TCA henceforth) in terms of impulse response analysis. Not only do we formulate TCA as a decomposition of total effects obtained through impulse response analysis, we rigorously establish that the calculation of impulse responses between different variables in the system is sufficient for the analysis of all transmission channels. Importantly, we also prove that only a single shock driving the impulse responses – the initial shock of interest – has to be structurally identified, and reduced-form impulse responses otherwise suffice. Consequently, TCA can be performed under the same conditions as traditional impulse response analysis, only requiring a structural identification scheme for a single shock plus a specified dynamic model. We prove that this equivalence holds for a large class of dynamic models, including structural vector autoregressive (SVAR) and linearised dynamic stochastic general equilibrium (DSGE) models.

Our third contribution is of a more technical nature. In order to develop the results discussed above, we develop a graphical approach to study transmission channels. Specifically, we show how to connect the impulse-response-space representation of the (structural) model’s equilibrium dynamics to a Directed Acyclic Graph (DAG). This involves a re-parameterisation of the dynamic equilibrium representation, which allows us to uniquely define a transmission channel as a collection of paths along the graph, connecting causal effects from one variable (resp. shock) to another variable and over time. To complement the graphical framework, we also develop an alternative representation of transmission channels in terms of potential outcomes. We prove that both representations are equivalent implying that transmission channels can be defined either as paths through

a graph or as a specific potential outcome. Apart from this specific result that is used throughout our theoretical analysis, the graphical and potential outcomes frameworks are of interest in themselves for the analysis of dynamic causal effects beyond our specific transmission questions.

Our final contribution is to illustrate the empirical usefulness of the framework for the purpose of policy evaluation. We study transmission channels in three distinct, well-established, empirical macroeconomic models that highlight the versatility of our approach. First, we investigate the prominent monetary policy shock series proposed by Romer and Romer (2004) and Gertler and Karadi (2015). Our transmission channels confirm the hypothesis (cf. McKay & Wolf, 2023) that the former appears to capture instantaneously implemented changes in the policy instrument, while the latter mostly picks up the forward guidance component. Second, we use TCA to shed light on anticipation effects of fiscal policy news. Using the military spending news series of Ramey and Zubairy (2018), we distinguish between anticipation effects and implementation effects by defining an anticipation channel as the effect of the news shock that is not driven by the response of government military spending. Third, we study transmission channels in the DSGE model of Smets and Wouters (2007). Here we decompose monetary policy effects on inflation through an interest rate channel, an expectation channel, and an output-wage channel.

Our paper touches upon various strands of academic literature. First, as already alluded to above, it is most closely related to the macroeconometric literature on the analysis of dynamic causal effects and (informal) transmission channels. For example, Gertler and Karadi (2015) infer qualitatively to what extent the effects of monetary policy are driven by credit costs by studying the impulse responses of term premia and credit spreads to monetary policy shocks. Similarly, impulse responses of various variables to government spending or tax (news) shocks are investigated to understand the transmission mechanisms of fiscal policies. For example, Ramey (2011) infers from the response of components of aggregate private consumption the importance of the wealth effect of spending shocks. Mertens and Ravn (2013), on the other hand, study the transmission mechanism for different types of tax changes, finding that cuts in personal and corporate income taxes both boost output via the investment channel, whereas only personal income cuts drive aggregate demand via an expansion in private consumption. Contrary to those qualitative approaches, we provide a logically coherent methodology to define and quantitatively assess the strength of transmission channels.

A related stream of literature uses impulse response analysis for studying coun-

terfactual questions (see e.g. Kilian & Lewis, 2011; McKay & Wolf, 2023; Sims & Zha, 2006). While transmission channel and counterfactual analysis superficially appear to be related, it is important to highlight their fundamental difference. Investigating counterfactual questions requires the researcher to specify a different model, describing a different equilibrium, where specific behavioural changes result in the counterfactual scenario. TCA, however, focuses on decomposing impulse responses within a given equilibrium rather than understanding the difference between responses across different equilibria. Therefore, TCA evaluates the relative importance of specific variables in transmitting the total effect of a particular identified economic shock, whereas counterfactual analysis investigates total causal effects that such shocks would have, had the policy response been different. As such, TCA complements counterfactual analysis; indeed, TCA can be used within a counterfactual study to investigate transmission channels across the different equilibria induced by the counterfactual behavioural rules.

TCA also shares similarities with mediation analysis (see, for example, Chan et al., 2016; Daniel et al., 2015; Hayes, 2018; Imai et al., 2010; Pearl, 2012) as it investigates causal effects going through intermediate variables. In contrast to TCA, mediation analysis focuses on causal models that do not exhibit any feedback mechanisms, limiting its usefulness for studying transmission channels in dynamic general equilibrium macroeconomics.

The use of DAGs for transmission channel analysis is related to the graphical causal analysis literature within computer science (see Pearl, 2009). Contrary to that literature, we do not require that the causal system - the set of behavioural equations - can be cast in a DAG. Instead, we show that for a large class of linear macroeconomic models, there always exists a DAG representation of the equilibrium equations rather than of the behavioural equations. This DAG representation, obtained using a QL-decomposition of the contemporaneous matrix, is related to the orthogonal reduced-form parameterisation of Arias et al. (2018). Importantly, this allows us to cover non-recursive models which exhibit contemporaneous feedback effects.

Finally, our work relates to the recent literature which uses potential outcomes in macroeconomics to gain more insights into total causal effects. Rambachan and Shephard (2021) use potential outcomes to investigate the non-parametric meaning of common macroeconomic causal estimands. Cloyne et al. (2023) use potential outcomes to investigate state dependent causal effects. Lastly, Angrist et al. (2018) use potential outcomes to estimate the effect of monetary policy semi-parametrically. Contrary to the aforementioned, our focus is on the decomposition

of total effects rather than on total effects themselves.

The paper is organised as follows. Section 2 contains an example of a simple three-variable system illustrating the main ideas behind TCA. The general TCA framework is then developed in Section 3. Section 4 contains our main theoretical results, while Section 5 applies the framework empirically to three different macroeconomic models. Section 6 concludes, while supplementary results are contained in the appendix.

2 TCA: An Illustrative Example

We present the main idea and intuition behind TCA using a textbook version of the three-equation New Keynesian model (Galí, 2015) including the output gap x_t , inflation π_t and nominal interest rates i_t . The model is given by

$$\begin{aligned} \text{IS: } \quad x_t &= \mathbb{E}[x_{t+1}] + \alpha_1(\boldsymbol{\theta})[i_t - \mathbb{E}[\pi_{t+1}]] + \varepsilon_t^d \\ \text{PC: } \quad \pi_t &= \mathbb{E}[\pi_{t+1}] + \alpha_2(\boldsymbol{\theta})x_t + \varepsilon_t^s \\ \text{MR: } \quad i_t &= \alpha_3 x_t + \alpha_4 \pi_t + \varepsilon_t^i, \end{aligned} \tag{1}$$

and consists of an IS equation and a Phillips curve (PC) equation, together summarising the equilibrium in the goods market, as well as a (Taylor-type) rule specifying the central bank's interest rate policy (MR). The coefficients of the IS and PC equations, α_1 and α_2 , depend on deep structural parameters $\boldsymbol{\theta}$ that specify the behaviour of firms and consumers in the economy. The coefficients of the interest rate rule, α_3 and α_4 , have a behavioural interpretation since they explicitly specify the policy of the central bank. The set of deep structural parameters in the model is thus $\boldsymbol{\vartheta} = \{\boldsymbol{\theta}, \alpha_3, \alpha_4\}$. The demand, supply and interest rate shocks are respectively given by ε_t^d , ε_t^s and ε_t^i .

For ease of exposition, we assume that the structural shocks ε_t^d , ε_t^s and ε_t^i are white noise and mutually uncorrelated. The equilibrium in (1) then exhibits the static representation

$$\underbrace{\begin{bmatrix} 1 & 0 & -\alpha_1(\boldsymbol{\theta}) \\ -\alpha_2(\boldsymbol{\theta}) & 1 & 0 \\ -\alpha_3 & -\alpha_4 & 1 \end{bmatrix}}_A \underbrace{\begin{bmatrix} x_t \\ \pi_t \\ i_t \end{bmatrix}}_{\mathbf{y}_t} = \underbrace{\begin{bmatrix} \varepsilon_t^d \\ \varepsilon_t^s \\ \varepsilon_t^i \end{bmatrix}}_{\boldsymbol{\varepsilon}_t}. \tag{2}$$

A core task of macroeconomists is to assess dynamic causal effects of structural shocks on relevant, endogenously determined economic variables. Generally the

focus is on *total* effects, i.e. total changes in equilibrium quantities triggered by an economically interpretable exogenous event. Since model (2) is static, total effects of structural shocks die out after a single period, and impact effects of the three structural shocks are summarised by the columns of the impulse response matrix

$$\Phi(\vartheta) = \begin{bmatrix} \frac{1}{\eta(\vartheta)} & \frac{\alpha_1(\boldsymbol{\theta})\alpha_4}{\eta(\vartheta)} & \frac{\alpha_1(\boldsymbol{\theta})}{\eta(\vartheta)} \\ \frac{\alpha_2(\boldsymbol{\theta})}{\eta(\vartheta)} & \frac{1-\alpha_1(\boldsymbol{\theta})\alpha_3}{\eta(\vartheta)} & \frac{\alpha_1(\boldsymbol{\theta})\alpha_2(\boldsymbol{\theta})}{\eta(\vartheta)} \\ \frac{\alpha_2(\boldsymbol{\theta})\alpha_4+\alpha_3}{\eta(\vartheta)} & \frac{\alpha_4}{\eta(\vartheta)} & \frac{1}{\eta(\vartheta)} \end{bmatrix},$$

where $\eta(\vartheta) = -\alpha_1(\boldsymbol{\theta})\alpha_2(\boldsymbol{\theta})\alpha_4 - \alpha_1(\boldsymbol{\theta})\alpha_3 + 1$.

The total effect (TE) of a demand shock on interest rates, quantitatively given by

$$\text{(TE)} \quad \Phi(\vartheta)_{3,1} = (\alpha_2(\boldsymbol{\theta})\alpha_4 + \alpha_3)/\eta(\vartheta), \quad (3)$$

can be decomposed into two *transmission channels*. The first channel, labelled the *indirect transmission channel*, measures how much of the interest rate response to a demand shock can be explained by the response of inflation to a demand shock *ceteris paribus*, i.e. holding all other endogenous and exogenous variables constant. The second channel, labelled the *direct transmission channel*, is the remainder of the total effect that is not explained by the indirect channel. It measures how much of the interest rate response to a demand shock cannot be explained *ceteris paribus* by the response in inflation to the demand shock.¹

Throughout, we take the deep structural parameterisation ϑ as given. This is contrary to counterfactual analysis where changes in total effects $\Phi(\vartheta)$ are analysed under changes in deep structural parameters ϑ , hence under different equilibria. By taking ϑ and thus the dynamic equilibrium representation as given, TCA focuses on explaining the effects within a specific equilibrium rather than understanding effects across different equilibria. TCA is therefore, by definition, not subject to the Lucas Critique. To keep notation simple, we subsequently suppress the dependence of α_1 and α_2 on $\boldsymbol{\theta}$. Furthermore, we first discuss TCA under simplified equilibrium dynamics ($\alpha_1(\boldsymbol{\theta}) = 0$) in Section 2.1 before turning to the more general equilibrium dynamics ($\alpha_1(\boldsymbol{\theta}) \neq 0$) in Section 2.2.

¹In the following, for brevity we suppress explicitly mentioning the *ceteris paribus* condition, but it should be kept in mind that this is intended when we discuss effects.

2.1 A Recursive Model

Consider model (2) with $\alpha_1 = 0$ which then implies that \mathbf{A} is lower-triangular; we label this the *recursive* (R) model. Equilibrium dynamics of the output gap are fully determined by the demand shock and the demand shock's total effect on interest rates is given by $\alpha_2\alpha_4 + \alpha_3$.

In this model there exist two *transmission channels* that jointly explain the total effect. First, the direct transmission channel consists of the effect of the demand shock on the output gap which is directly carried forward to interest rates. Second, the indirect transmission channel consists of the effect of the demand shock on the output gap, which is carried forward to inflation and in turn to interest rates.

TCA quantifies the effect that goes through each transmission channel, the *transmission effect*. To simplify this task, we cast the analysis of transmission channels in a graphical framework by connecting the model to an associated Directed Acyclic Graph (DAG), as visualised in Figure 1 panel (R). The three key ingredients of the graph are the nodes, edges, and path coefficients. The nodes represent either the variables in the model (solid black circles) or the shocks (shaded blue squares). The edges are directed and represent the effects. Edges originating from shocks represent causal effects; their path coefficient represents the direct causal effect size of the structural shock on the destination variable. Edges originating from variables we label as carrying effects since they carry the causal effect forward; their path coefficients quantify the direct effect of a unit increase in the origin variable (irrespective of what drove this increase) on the destination variable.

We aim to decompose the total effect of the demand shock ε_t^d on interest rates (TE, $\alpha_2\alpha_4 + \alpha_3$) into *direct effects* (DE) and *indirect effects* (IE) that go through the direct and indirect channels respectively. The total effect ($\alpha_2\alpha_4 + \alpha_3$) can be read of Figure 1 panel (TE) by multiplying the path coefficients of the edges along each path from ε_t^d to i_t and then adding up the results across all paths. The direct channel is visualised in Figure 1 panel (DE), the indirect channel in panel (IE). Transmission effects can be read from the graph in a similar way as the total effect. The transmission effects of the direct and indirect channel are respectively given by

$$\text{(DE)} \quad \alpha_3, \quad \text{(IE)} \quad \alpha_2\alpha_4. \quad (4)$$

The transmission effects of the disjoint direct and indirect channels thus add up to the total effect; thereby decomposing the total effect.

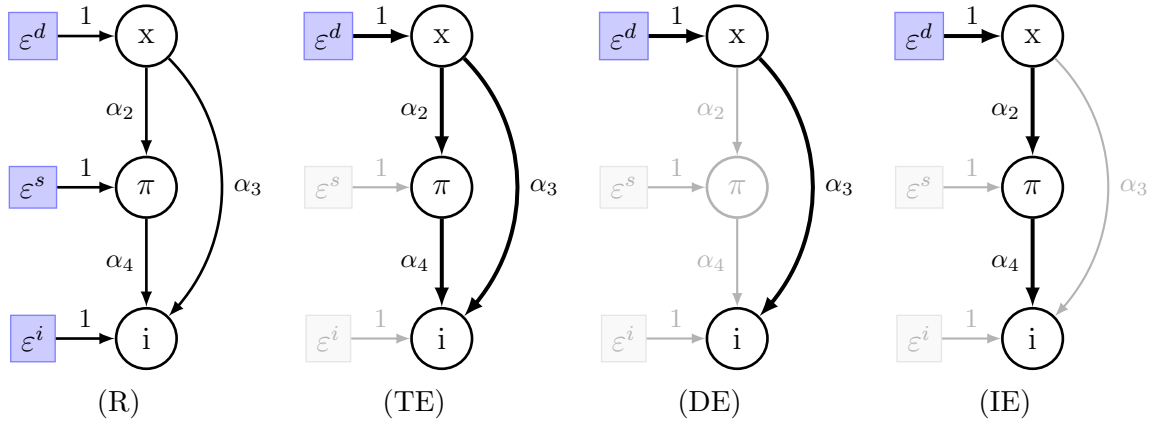


Figure 1: Illustrative recursive example (R). We analyse the total effect (TE) of a demand shock on interest rates, which is decomposed into a direct (DE) and indirect effect (IE) through inflation. Gray nodes and edges are irrelevant for the effect shown in each panel.

2.2 The Non-Recursive Model

Consider the general three-equation New Keynesian model (2) with $\alpha_1 \neq 0$. The contemporaneous matrix \mathbf{A} is no-longer lower-triangular; the model is now *non-recursive* (NR). Equilibrium dynamics of the output gap are no-longer fully determined by the demand shock, as visualised in Figure 2 panel (NR) by two incoming edges into x_t . This complicates the equilibrium dynamics and TCA cannot be performed directly on this graph since the feedback loop (or cycle) between the output gap and inflation in Figure 2 panel (NR) implies that no logically consistent definition of a transmission channel exists.

While simply restricting α_1 to zero would break the cycle in the graph, it would also change the equilibrium since it would require an explicit change in the deep structural parameters ϑ . Restricting $\alpha_1 = 0$ would thus correspond to a counterfactual analysis, comparing the total dynamic effect across two equilibria; one equilibrium under $\alpha_1 \neq 0$ and one under $\alpha_1 = 0$. TCA, in contrast, takes ϑ and thus the dynamic equilibrium representation as given. To decompose the equilibrium dynamics leading to the total effects, TCA requires model (2) to be re-parameterised into an equivalent equilibrium representation that lends itself to logically consistent definitions of transmission channels - a parameterisation that does not involve a feedback loop (cycle) and that can then be represented by a DAG.

Since our focus is on the transmission of shocks in an equilibrium representation, any equivalent equilibrium representation can be used that permits the

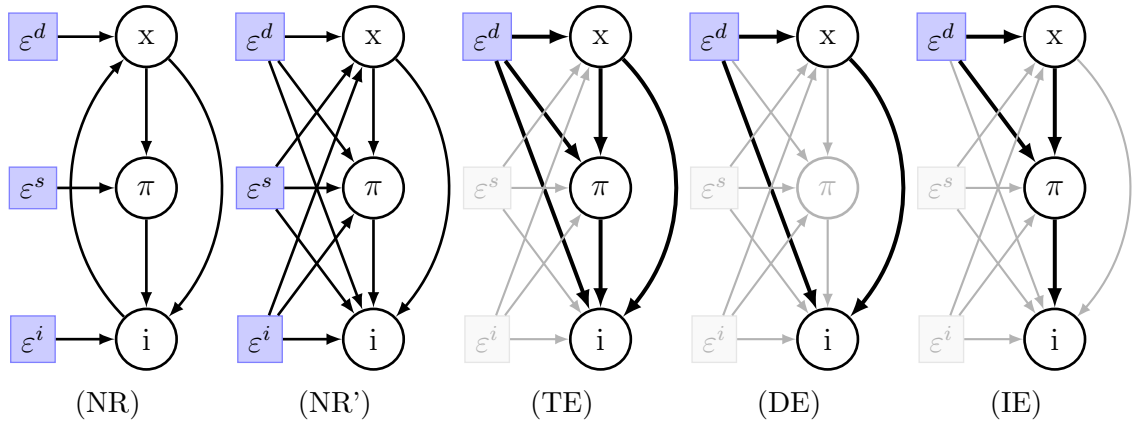


Figure 2: Illustrative non-recursive example (NR) together with the re-parameterised acyclic graph suitable for TCA (NR'). We analyse the total effect (TE) of a demand shock on interest rates, which is decomposed into a direct (DE) and indirect effect (IE) through inflation. Gray nodes and edges are irrelevant for the effect shown in each panel.

quantification of the transmission channels of interest. The re-parameterisation step is therefore crucially determined by the research question. To quantify the effect corresponding to the direct and indirect transmission channel, we seek a representation of the form

$$\mathbf{L} \begin{bmatrix} x_t \\ \pi_t \\ i_t \end{bmatrix} = \mathbf{Q}' \begin{bmatrix} \varepsilon_t^d \\ \varepsilon_t^s \\ \varepsilon_t^i \end{bmatrix}, \quad (5)$$

where equilibrium interest rates depend on inflation and the output gap; here \mathbf{L} is a lower-triangular matrix and \mathbf{Q} is a rotation matrix. Model (5) describes the same dynamic equilibrium as model (2) and is suitable to perform TCA for the research question at hand, but the interpretation of individual equations may be different and the re-parameterised relationships among variables may no longer have a behavioural interpretation. For example, the re-parameterised formulation of the “inflation equation” and the “interest rate equation” may now include the demand shock; and the re-parameterised relationship between the interest rate and inflation does not characterise the central bank’s policy reaction anymore.

Representation (5) can be obtained using a QL-decomposition of the matrix \mathbf{A} which specifies the contemporaneous relationships among the endogenous variables. Multiplying both sides of (5) by \mathbf{Q} and noting that $\mathbf{Q}\mathbf{Q}' = \mathbf{I}$, we obtain

$$\mathbf{QL} \begin{bmatrix} x_t \\ \pi_t \\ i_t \end{bmatrix} = \begin{bmatrix} \varepsilon_t^d \\ \varepsilon_t^s \\ \varepsilon_t^i \end{bmatrix}$$

where $\mathbf{A} = \mathbf{QL}$ is unique given a variable ordering and assuming that \mathbf{A} is non-singular.

Model (5) can now be represented as a DAG, see Figure 2 panel (NR') with path coefficients omitted for clarity. Unlike to the DAG of Section 2.1, edges now exist from all shocks to all variables. Focusing on the total effect of the demand shock on interest rates in Figure 2 (TE), edges exist from the demand shock to the output gap, as before, but also to inflation and interest rates; their interpretation remains the same as in Section 2.1. There are two paths from the demand shock to the output gap not going through inflation that form the direct transmission channel in Figure 2 (DE) and two paths going through inflation that together form the indirect channel in Figure 2 (IE). The corresponding transmission effects can be computed as before and are respectively given by

$$\begin{aligned} \text{(DE)} \quad & (\alpha_3 + \alpha_1(1 - \eta))/((1 + \alpha_1^2)\eta) \\ \text{(IE)} \quad & (\alpha_2\alpha_4)/((1 + \alpha_1^2)\eta). \end{aligned} \tag{6}$$

Finally, note that the transmission channels and effects obtained through model (5) depend on the ordering of the variables in the QL-decomposition. Importantly, this ordering is not needed to identify the structural shock of interest and its meaning is therefore fundamentally different from the ordering for the Cholesky decomposition in recursively identified structural models. Instead, it is required to quantify the transmission channels of interest, as determined entirely by the research question. Given its crucial role for TCA, we encode this variable ordering in a permutation matrix \mathbf{T} which we label the *transmission matrix*.

Figure 3 gives all possible permutations of the transmission matrix in the example of this section. With $\mathbf{A}^* = \mathbf{AT}'$ and $\mathbf{y}_t^* = \mathbf{T}\mathbf{y}_t$, the QL-decomposition of \mathbf{A}^* results in six equivalent equilibrium representations, whose DAG representations are visualised in panels (a) to (f). The choice of transmission matrix determines the possible paths through the DAG and therefore transmission channels up for analysis. To answer our research question we need an equilibrium representation in which the interest rate depends on inflation and the output gap. This holds for the transmission matrices \mathbf{T} in panels (a) and (c), thereby directly ruling out the choice of \mathbf{T} in the other panels. By ordering the output gap before inflation as in panel (a), we also enforce that inflation is dependent on the output gap, making it the only natural and logical choice to quantify our two transmission effects of interest.

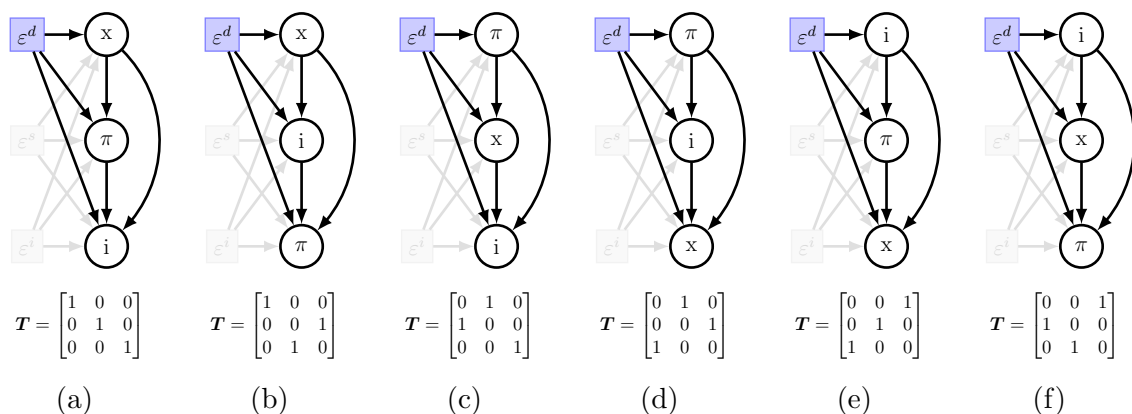


Figure 3: Panels (a) through (f) show all possible permutations of the three variables x_t , π_t and i_t as encoded in the transmission matrix \mathbf{T} . The associated DAG is shown above the matrix where gray nodes and edges are irrelevant for the transmission of a demand shock.

3 The General Framework

In this section we formalise the intuition developed in the previous section. Section 3.1 introduces the general dynamic model we consider together with its impulse-response representation we use to compute total effects. Section 3.2 then introduces the associated DAG which we use to decompose the total effect into transmission channels, and formally defines transmission channels and transmission effects.

3.1 Dynamic Models and Total Effects

For our general setup, we assume \mathbf{y}_t to be a K -dimensional stationary stochastic process with a structural Vector Autoregressive Moving Average (VARMA) representation given by

$$\mathbf{A}_0 \mathbf{y}_t = \sum_{i=1}^{\ell} \mathbf{A}_i \mathbf{y}_{t-i} + \sum_{j=1}^q \boldsymbol{\Psi}_j \boldsymbol{\varepsilon}_{t-j} + \boldsymbol{\varepsilon}_t, \quad (7)$$

where $\{\mathbf{A}_i\}_{i=1}^{\ell}$ and $\{\boldsymbol{\Psi}_j\}_{j=1}^q$ are $K \times K$ coefficient matrices which are statistically identified using any common scheme such as the echelon form (e.g., Poskitt, 1992), \mathbf{A}_0 is a contemporaneous coefficient matrix assumed to be (partially) identified using some economic identification scheme, and $\boldsymbol{\varepsilon}_t$ is a $K \times 1$ vector of white noise.

The structural VARMA model (7) encompasses a wide range of popular dynamic models used in macroeconomic research. The SVAR is recovered by setting $\boldsymbol{\Psi}_j = \mathbf{0}$ (for $j = 1, \dots, q$), while linearised DSGE models can be represented as

structural VARMA with cross-equation restrictions (Fernández-Villaverde et al., 2007; Ravenna, 2007).

We make two standard assumptions on ε_t and \mathbf{A}_0 .

Assumption 1. The white noise vector ε_t consists of K structural shocks satisfying $\mathbb{E}[\varepsilon_t] = \mathbf{0}_K$, $\mathbb{E}[\varepsilon_t \varepsilon_t'] = \mathbf{I}_K$ and $\mathbb{E}[\varepsilon_t \varepsilon_{t-r}'] = \mathbf{O}_K$ for all $r \geq 1$.

Assumption 2. \mathbf{A}_0 is non-singular.

Assumption 1 assures that impulse responses with respect to the white noise disturbances ε_t have a causal interpretation. Assumption 2 then assures that these causally interpretable impulse responses can be obtained from reduced-form impulse response functions. Section 4.2 uses this last implication to show how transmission effects can be obtained from a single identified shock. Hence, \mathbf{A}_0 may be only partially identified.

While all equivalent equilibrium representations can be used to analyse total effects, their decomposition into transmission channels requires a precise definition of which variables depend on which other variables in equilibrium. TCA thus involves choosing the ordering of variables using the transmission matrix \mathbf{T} .

Definition 1. The *transmission matrix* \mathbf{T} denotes the $K \times K$ permutation matrix defining the ceteris paribus dependencies of the K variables in the chosen equilibrium representation; it is fixed and specified by the researcher.

Having a fixed and completely specified transmission matrix assures a fixed equilibrium representation. However, Section 4.2 shows that, under certain conditions when two distinct transmission matrices lead to the same transmission effect, the transmission matrix only needs to be partially specified, so only a partial variable ordering is required in such case.

Under the conditions formulated above, the QL-decomposition of $\mathbf{A}_0^* = \mathbf{A}_0 \mathbf{T}'$ is unique, implying that the structural VARMA (7) can be written in unique lower-triangular form

$$\mathbf{L} \mathbf{y}_t^* = \sum_{i=1}^{\ell} \mathbf{Q}' \mathbf{A}_i^* \mathbf{y}_{t-i}^* + \sum_{j=1}^q \mathbf{Q}' \Psi_j \varepsilon_{t-j} + \mathbf{Q}' \varepsilon_t, \quad (8)$$

where \mathbf{L} is a $K \times K$ lower-triangular matrix, $\mathbf{y}_t^* = \mathbf{T} \mathbf{y}_t$, $\mathbf{A}_i^* = \mathbf{A}_i \mathbf{T}'$ for $i = 1, \dots, \ell$ and \mathbf{Q} is a $K \times K$ rotation matrix.

Throughout the paper, we focus on transmission channels of the total effect of shock $\varepsilon_{i,t}$ to $y_{j,t+h}^*$ over the fixed finite impulse-response horizon h . Then the lower-triangular form (8) can be re-written in systems form, capturing all dynamics of

the shock $\varepsilon_{i,t}$ up to horizon h . Defining $\mathbf{x} = (\mathbf{y}_t^*, \dots, \mathbf{y}_{t+h}^*)'$ and $\boldsymbol{\varepsilon} = (\varepsilon_t', \dots, \varepsilon_{t+h}')'$, the systems form is given by

$$\mathbf{x} = \mathbf{B}\mathbf{x} + \boldsymbol{\Omega}\boldsymbol{\varepsilon}, \quad (9)$$

where \mathbf{B} is lower-triangular with zeros on the diagonal, $\boldsymbol{\Omega}$ is lower-block-triangular, and both are respectively given by²

$$\mathbf{B} = \begin{bmatrix} \mathbf{I} - \mathbf{DL} & \mathbf{O} & \dots & \mathbf{O} \\ \mathbf{DQ}'\mathbf{A}_1^* & \mathbf{I} - \mathbf{DL} & \dots & \mathbf{O} \\ \vdots & \ddots & \ddots & \vdots \\ \mathbf{DQ}'\mathbf{A}_h^* & \dots & \mathbf{DQ}'\mathbf{A}_1^* & \mathbf{I} - \mathbf{DL} \end{bmatrix}, \quad \boldsymbol{\Omega} = \begin{bmatrix} \mathbf{DQ}' & \mathbf{O} & \dots & \mathbf{O} \\ \mathbf{DQ}'\boldsymbol{\Psi}_1 & \mathbf{DQ}' & \dots & \mathbf{O} \\ \vdots & \ddots & \ddots & \vdots \\ \mathbf{DQ}'\boldsymbol{\Psi}_h & \dots & \mathbf{DQ}'\boldsymbol{\Psi}_1 & \mathbf{DQ}' \end{bmatrix}, \quad (10)$$

with $\mathbf{D} = \text{diag}(\mathbf{L})^{-1}$, where $\text{diag}(\mathbf{X})$ is a diagonal matrix of the diagonal of \mathbf{X} , $\mathbf{A}_i^* = \mathbf{O}$ for $i > \ell$ and $\boldsymbol{\Psi}_j = \mathbf{O}$ for $j > q$; see Appendix A for further details.

The total effects can then be obtained from the impulse-response representation

$$\mathbf{x} = \boldsymbol{\Phi}\boldsymbol{\varepsilon}, \quad \boldsymbol{\Phi} = (\mathbf{I} - \mathbf{B})^{-1}\boldsymbol{\Omega}. \quad (11)$$

Under our assumptions the impulse response matrix $\boldsymbol{\Phi}$ always exists. The aim of TCA is to decompose these total effects into transmission channels. However, before turning to the graphical representation used for this decomposition, we first revisit the examples of Section 2 in our general framework.

Example 1. For the recursive model of Section 2.1, $\mathbf{T} = \mathbf{I}$, $\mathbf{B} = \mathbf{I} - \mathbf{DA}$ and $\boldsymbol{\Omega} = \mathbf{D}$ with $\mathbf{D} = \text{diag}(\mathbf{A})^{-1} = \mathbf{I}$. The total effect of ε_t^d on i_t is therefore $\alpha_2\alpha_4 + \alpha_3$.

Example 2. For the non-recursive model of Section 2.1 with transmission matrix $\mathbf{T} = \mathbf{I}$,

$$\mathbf{B} = \begin{bmatrix} 0 & 0 & 0 \\ \frac{(\alpha_1^2+1)\alpha_2+\alpha_1\alpha_4(1-\alpha_1\alpha_3)}{\alpha_1^2(\alpha_4^2+1)+1} & 0 & 0 \\ \frac{\alpha_1+\alpha_3}{\alpha_1^2+1} & \frac{\alpha_4}{\alpha_1^2+1} & 0 \end{bmatrix} \quad \text{and} \quad \boldsymbol{\Omega} = \begin{bmatrix} \frac{1}{1-\alpha_1(\alpha_2\alpha_4+\alpha_3)} & \frac{\alpha_1\alpha_4}{1-\alpha_1(\alpha_2\alpha_4+\alpha_3)} & \frac{\alpha_1}{1-\alpha_1(\alpha_2\alpha_4+\alpha_3)} \\ -\frac{\alpha_1\alpha_4}{\alpha_1^2(\alpha_4^2+1)+1} & \frac{\alpha_1^2+1}{\alpha_1^2(\alpha_4^2+1)+1} & -\frac{\alpha_1\alpha_4}{\alpha_1^2(\alpha_4^2+1)+1} \\ -\frac{\alpha_1}{\alpha_1^2+1} & 0 & \frac{1}{\alpha_1^2+1} \end{bmatrix}.$$

The total effect of ε_t^d on i_t is therefore $(\alpha_2\alpha_4 + \alpha_3)/\eta$, where $\eta = -\alpha_1\alpha_2\alpha_4 - \alpha_1\alpha_3 + 1$.

²Note that $\mathbf{I} = \mathbf{I}_K$ and $\mathbf{O} = \mathbf{O}_K$. For expositional simplicity, we henceforth omit the dimension subscript.

3.2 Dynamic Graphs and Transmission Channels

To decompose the total effects given by Φ in equation (11) into transmission channels, we introduce the graph $\mathcal{G}(\mathbf{B}, \mathbf{\Omega})$ associated with system (9). The graph $\mathcal{G}(\mathbf{B}, \mathbf{\Omega})$ is a DAG and has three key ingredients: nodes, directed edges and path coefficients. A node exists for each shock $\varepsilon_{i,r}$ at time $r = t$ and for each variable $y_{i,r}$ at time points $r = t, \dots, t+h$, where h is the fixed horizon. Let $\mathbf{x} = (\mathbf{y}_t^*, \dots, \mathbf{y}_{t+h}^*)'$ and $\boldsymbol{\varepsilon} = (\boldsymbol{\varepsilon}'_t, \dots, \boldsymbol{\varepsilon}'_{t+h})'$ as in equation (9). A directed edge $x_i \rightarrow x_j$ then exists between variable x_i and variable x_j whenever $\mathbf{B}_{j,i} \neq 0$, where $\mathbf{B}_{j,i}$ denotes the (j, i) element of \mathbf{B} . The path coefficient of this edge is given by $\omega_{x_i, x_j} = \mathbf{B}_{j,i}$ and is interpreted as the direct effect of a unit increase in x_i (irrespective of the cause) on x_j . Similarly, a directed edge $\varepsilon_i \rightarrow x_j$ exists from the structural shock ε_i to the variable x_j whenever $\boldsymbol{\Omega}_{j,i} \neq 0$. The path coefficient of this edge is given by $\omega_{\varepsilon_i, x_j} = \boldsymbol{\Omega}_{j,i}$ and is similarly interpreted as the direct causal effect of a unit increase in ε_i on x_j .

Example 3. Consider the trivariate SVAR(1) given by

$$\mathbf{A}_0 \mathbf{y}_t = \mathbf{A}_1 \mathbf{y}_{t-1} + \boldsymbol{\varepsilon}_t,$$

with \mathbf{A}_0 and \mathbf{A}_1 being 3×3 coefficient matrices, $\mathbf{y}_t = (y_{1,t}, y_{2,t}, y_{3,t})'$ and $\boldsymbol{\varepsilon}_t = (\varepsilon_{1,t}, \varepsilon_{2,t}, \varepsilon_{3,t})'$. Fixing the horizon $h = 1$ and the transmission matrix $\mathbf{T} = \mathbf{I}$,

$$\begin{aligned} \mathbf{x} &= (y_{1,t}, y_{2,t}, y_{3,t}, y_{1,t+1}, y_{2,t+1}, y_{3,t+1})' \\ \boldsymbol{\varepsilon} &= (\varepsilon_{1,t}, \varepsilon_{2,t}, \varepsilon_{3,t}, \varepsilon_{1,t+1}, \varepsilon_{2,t+1}, \varepsilon_{3,t+1})', \end{aligned}$$

and the corresponding graph $\mathcal{G}(\mathbf{B}, \mathbf{\Omega})$ is shown in Figure 4(a). Due to the dynamic nature of the SVAR(1), an edge exists from each component of \mathbf{y}_t (i.e. x_1 to x_3 in the graph) to each component of \mathbf{y}_{t+1} (i.e. x_4 to x_6 in the graph).

Example 4. Assume, instead of a trivariate SVAR(1), a trivariate SVARMA(1, 1)

$$\mathbf{A}_0 \mathbf{y}_t = \mathbf{A}_1 \mathbf{y}_{t-1} + \boldsymbol{\varepsilon}_t + \boldsymbol{\Psi}_1 \boldsymbol{\varepsilon}_{t-1},$$

with \mathbf{A}_0 , \mathbf{A}_1 and $\boldsymbol{\Psi}_1$ being 3×3 coefficient matrices, $\mathbf{y}_t = (y_{1,t}, y_{2,t}, y_{3,t})'$ and $\boldsymbol{\varepsilon}_t = (\varepsilon_{1,t}, \varepsilon_{2,t}, \varepsilon_{3,t})'$. Fixing the horizon $h = 1$ and the transmission matrix $\mathbf{T} = \mathbf{I}$, \mathbf{x} and $\boldsymbol{\varepsilon}$ are the same as in Example 3, but the graph is given in Figure 4(b). Similar to the graph corresponding to the SVAR(1), edges exist from each component of \mathbf{y}_t to each component of \mathbf{y}_{t+1} . Unlike the SVAR case, edges from structural shocks can now also skip time periods, thereby going from each component of $\boldsymbol{\varepsilon}_t$ to each

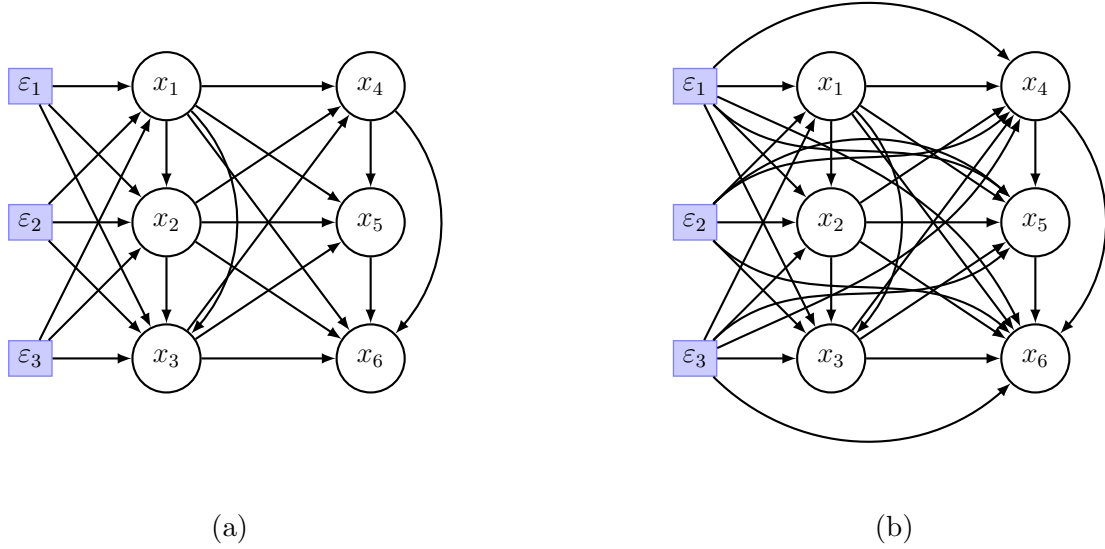


Figure 4: Panels (a) and (b) show the DAG corresponding to a SVAR(1) and a SVARMA(1, 1) respectively, where $\mathbf{x} = (y_{1,t}, y_{2,t}, y_{3,t}, y_{1,t+1}, y_{2,t+1}, y_{3,t+1})'$. Compared to panel (a), panel (b) has edges from all shocks $\varepsilon_{\cdot,t}$ to all variables in period $t + 1$, $y_{\cdot,t+1}$, where \cdot is used as a placeholder.

component of \mathbf{y}_{t+1} . One such edge is given by $\varepsilon_1 \rightarrow x_4$, which is still interpreted as a direct causal effect of a unit increase in ε_1 on x_4 .

Since each edge describes a direct effect, paths – consisting of chained edges – can be interpreted as descriptions of causal flows. The collection $\mathcal{P}_{\varepsilon_i, x_j}$ of all paths connecting the structural shock ε_i to the variable x_j is thus a set of causal descriptions; so is any subset P_{ε_i, x_j} of this collection. We are now ready to define a transmission channel.

Definition 2. Let $\mathcal{G}(\mathbf{B}, \boldsymbol{\Omega})$ be the graph induced by model (9). A subset of paths from ε_i to x_j , $P_{\varepsilon_i, x_j} \subset \mathcal{P}_{\varepsilon_i, x_j}$, is called a *transmission channel*.

Through TCA we quantify transmission effects as the effects flowing through transmission channels. To this end, we define the effects along a specific path p and the effects along a collection of paths P_{ε_i, x_j} , the latter of which leads to the definition of the transmission effect.

Definition 3. Let $\mathcal{G}(\mathbf{B}, \boldsymbol{\Omega})$ be a graph induced by model (9), $\mathcal{P}_{\varepsilon_i, x_j}$ be the collection of all paths in $\mathcal{G}(\mathbf{B}, \boldsymbol{\Omega})$ from ε_i to x_j , and ξ be the shock size.

1. The *path-specific effect* of a path $p \in \mathcal{P}_{\varepsilon_i, x_j}$ is

$$Q_\xi(p) = \xi \sum_{u \rightarrow v \in p} \omega_{u,v},$$

where $\omega_{u,v}$ is the path coefficient of the edge going from node u to node v on path p .

2. The *total path-specific effect* of a sub-collection of paths $P_{\varepsilon_i, x_j} \subseteq \mathcal{P}_{\varepsilon_i, x_j}$ is

$$\mathcal{Q}_\xi(P_{\varepsilon_i, x_j}) = \sum_{p \in P_{\varepsilon_i, x_j}} \mathcal{Q}_\xi(p).$$

3. The *transmission effect* of the transmission channel $P_{\varepsilon_i, x_j} \subset \mathcal{P}_{\varepsilon_i, x_j}$ is the total path-specific effect of P_{ε_i, x_j} .

Example 1 (continued). The graph $\mathcal{G}(\mathbf{B}, \boldsymbol{\Omega})$ corresponding to the recursive model of Section 2.1 is given in Figure 1 panel (R). Due to its recursive nature, all shocks have only a single directed edge to one variable. The indirect effect of ε_t^d through π_t onto i_t , in Figure 1 panel (IE), is given by the set of paths $P_{\varepsilon_t^d, i_t} = \{\varepsilon_t^d \rightarrow x_t \rightarrow \pi_t \rightarrow i_t\}$ with total path-specific effect $\mathcal{Q}_1(P_{\varepsilon_t^d, i_t}) = \alpha_2 \alpha_4$. This is the transmission effect of the indirect transmission channel.

Example 2 (continued). The graph $\mathcal{G}(\mathbf{B}, \boldsymbol{\Omega})$ corresponding to the non-recursive model of Section 2.2 is given by Figure 2 panel (NR'). Due to its non-recursive nature, edges now exist from structural shocks to several variables. These direct edges are interpreted as direct causal effects of a unit increase in ε_t^d . The indirect effect of ε_t^d through π_t on i_t , in Figure 2 panel (IE), is now given by $P_{\varepsilon_t^d, i_t} = \{\varepsilon_t^d \rightarrow x_t \rightarrow \pi_t \rightarrow i_t, \varepsilon_t^d \rightarrow \pi_t \rightarrow i_t\}$. The total path-specific effect of $P_{\varepsilon_t^d, i_t}$, and thus the transmission effect of the indirect channel, is given by $\mathcal{Q}_1(P_{\varepsilon_t^d, i_t}) = (\alpha_2 \alpha_4) / ((1 + \alpha_1^2) \eta)$.

Given the formal definition of TCA in dynamic models (Definitions 2 and 3) for system (9) and its associated graph $\mathcal{G}(\mathbf{B}, \boldsymbol{\Omega})$, we now provide some intuition for our three main results that we formally prove in Section 4.2. For ease of exposition, consider a transmission channel P_{ε_i, x_j} of ε_i on x_j through x_k consisting of all paths starting at ε_i , going to x_k and ending in x_j . First, note that the total effect of ε_i on x_j equals the total path-specific effect of $\mathcal{P}_{\varepsilon_i, x_j}$. This ensures the coherence of our framework.

Second, transmission channels of the total effect of ε_i only require ε_i itself to be structurally identified. Edges leaving the structural shock ε_i are causal effects of ε_i , thereby requiring structural identification. Edges leaving any intermediate variable x_m on a path $p \in P_{\varepsilon_i, x_j}$, however, are effects of a unit increase in x_m , irrespective of the cause. Therefore, they do not require structural identification.

Thus, only the single edge on any path $p \in P_{\varepsilon_i, x_j}$ originating from ε_i requires structural identification.

Third, all transmission effects of transmission channels decomposing the total effect of ε_i on x_j can be calculated by combining the structural impulse responses of ε_i together with non-structural impulse responses; thus, impulse responses are sufficient for the calculation of any transmission effect. All paths p corresponding to the transmission channel P_{ε_i, x_j} go through the intermediate variable x_k , through which the transmission channel P_{ε_i, x_j} can be split. The first part consists of all paths connecting ε_i with x_k , while the second part consists of all paths connecting x_k to x_j . The first part is the total effect of ε_i on x_k obtained through the structural impulse response $\Phi_{k,i}$. The second part corresponds to the total effect of a unit increase in variable x_k on x_j ; in other words, the reduced-form impulse response. In the next section, we prove these three main findings making use of the potential outcomes framework.

4 Main Results

In this section, we establish four main results on TCA. To this end, we use the potential outcomes framework as a convenient mathematical tool. In Section 4.1, we introduce potential outcomes for TCA and show its equivalence with the graphical definitions and representation of TCA. In Section 4.2, we then show that (i) the total effect of ε_i on x_j is the total path-specific effect of $\mathcal{P}_{\varepsilon_i, x_j}$, (ii) IRFs are sufficient statistics to compute transmission effects since structural IRFs can be combined with IRFs obtained using a Cholesky decomposition to obtain any transmission effect, and (iii) only the shock of interest ε_i needs to be structurally identified for transmission effects to be identified. The proofs of all results are provided in Appendix B.

4.1 Transmission Effects as Potential Outcomes

We introduce potential outcomes for TCA by adapting notation used in the mediation analysis literature (Daniel et al., 2015). We show that the potential outcomes framework and the more intuitive, graphical framework for TCA used in Section 3 are equivalent. Throughout this section, we consider the effects from the structural shock ε_i to the variable x_j .

4.1.1 Notation

Recall system (9), $\mathbf{x} = \mathbf{B}\mathbf{x} + \mathbf{\Omega}\boldsymbol{\varepsilon}$. Since \mathbf{B} is lower-triangular with zeros on the diagonal, x_j directly depends on the realisations of x_i for $i < j$, which, in turn, directly depends on the realisations of x_k for $k < i$. All variables may, additionally, depend on realisations of the shock of interest ε_i . However, shocks themselves are independent of all other variables and shocks. Thus, chains can be traced back from the variable of interest x_j to the structural shock ε_i . Potential outcomes are statements about these chains, with the potential outcome for x_j taking the form

$$x_j(x_1(\epsilon_1), x_2(x_1(\epsilon_2), \epsilon_3), \dots) = x_j^*(\epsilon_1, \epsilon_2, \epsilon_3, \dots, \epsilon_{\eta(j)}) = x_j(\boldsymbol{\epsilon}^{(j)}),$$

where $\boldsymbol{\epsilon}^{(j)}$ is the potential outcomes assignment vector. The elements of this vector, ϵ_l for $l = 1 \dots \eta(j)$, are the realisations of the structural shock experienced by the l th nested chain, where $\eta(j) = 2^{j-1}$ is the number of chains moving back from x_j to ε_i .

Example 2 (continued). Consider the non-recursive model in equation (2) with associated graph in Figure 5 panel (a), where all except the demand shock have been omitted for clarity. The first step to introducing potential outcomes is to bring the model into general notation. Thus, $\varepsilon_1 = \varepsilon_t^d$, $x_1 = x_t$, $x_2 = \pi_t$ and $x_3 = i_t$, see Figure 5 panel (a'). The potential outcome for the interest rate x_3 is then given by

$$x_3(x_1(\epsilon_1), x_2(x_1(\epsilon_2), \epsilon_3), \epsilon_4) = x_3^*(\epsilon_1, \epsilon_2, \epsilon_3, \epsilon_4) = x_3^*(\boldsymbol{\epsilon}^{(3)}),$$

where ϵ_l ($l = 1, \dots, 4$) are the realisations of the structural shock ε_1 . Note that the different realisations of the structural shock do not have to be the same.

Figure 5 panels (b) to (e) depict the nested chains corresponding to the shock realisations ϵ_1 to ϵ_4 respectively. Panel (b) shows that x_3 depends on the realisation of x_1 , which, in turn, depends on a realisation of the structural shock ε_1 , denoted by ϵ_1 . Panels (c) and (d) both start from the dependence of x_3 on the realisation of x_2 . Panel (c) then considers the chain where x_2 depends on the realisation of x_1 , which in turn depends on the realisation of the structural shock ε_2 . Panel (d) considers the chain where x_2 depends on the realisation of the structural shock ε_3 . Lastly, panel (e) shows that x_3 directly depends on the realisation of the structural shock ε_4 .

As evident from the example, keeping track of the various dependencies and the corresponding shock realisations in the potential outcomes assignment vector

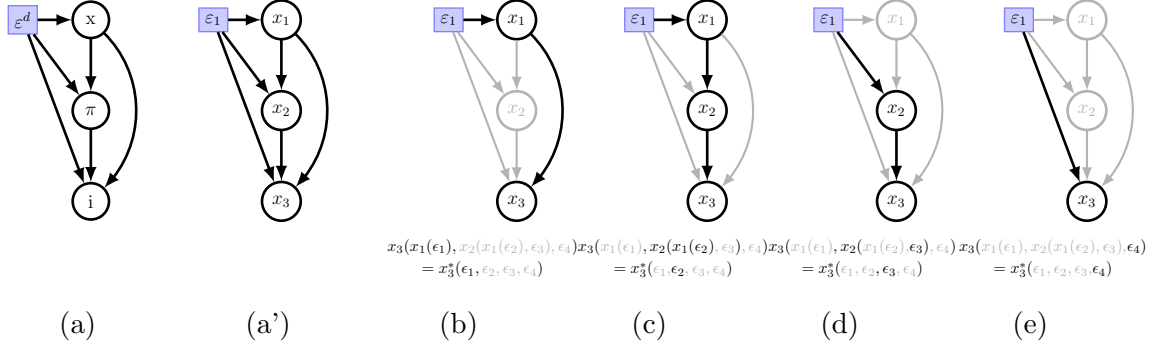


Figure 5: Panel (a) shows the DAG of the non-recursive model in Example 2 with all except the demand shock omitted, while panel (a') shows the same DAG but in general notation. Panels (b) through (e) show, on top, the paths (in black) corresponding to each element in the potential outcome and its assignment vector (highlighted in black below the graph).

$\epsilon^{(j)}$ quickly leads to notational clutter. For notational convenience, we therefore introduce additional indexing notation to keep track of elements in the assignment vector that correspond to dependencies involving certain intermediate variables. Defining $H(j) = 2^j - 1$, the entries $H(k_1 - 1) + 1$ to $H(k_1)$ in the assignment vector $\epsilon^{(j)}$ correspond to the dependencies of the variable of interest x_j on variable x_{k_1} , which we jointly collect in $\epsilon^{(j \cdot k_1)} = (\epsilon_{H(k_1-1)+1}^{(j)}, \dots, \epsilon_{H(k_1)}^{(j)})$. In the subset of dependencies of x_j on x_{k_1} , we can further single out the dependencies on another variable x_{k_2} , $k_2 < k_1$, that is ranked higher up in the system. Then $\epsilon^{(j \cdot k_1 \cdot k_2)}$ collects the entries in the assignment vector corresponding to the dependencies of x_j on x_{k_1} and x_{k_1} in turn on x_{k_2} . Continuing in this way, we thus define

$$\begin{aligned}
\epsilon^{(j)} &= (\epsilon_1, \dots, \epsilon_{\eta(j)}) \\
\epsilon^{(j \cdot k_1)} &= (\epsilon_{H(k_1-1)+1}^{(j)}, \dots, \epsilon_{H(k_1)}^{(j)}) \\
\epsilon^{(j \cdot k_1 \cdot k_2)} &= (\epsilon_{H(k_2-1)+1}^{(j \cdot k_1)}, \dots, \epsilon_{H(k_2)}^{(j \cdot k_1)}) \\
&\vdots
\end{aligned}$$

Example 2 (continued). Figure 5 panels (c) and (d) show the two nested dependencies of x_3 on the intermediate variable x_2 . The two elements in the potential outcomes assignment vector $\epsilon^{(3)}$ corresponding to the shock realisations experienced by these two nested dependencies are $\epsilon^{(3 \cdot 2)} = (\epsilon_2, \epsilon_3)$. We can then further single out the single element in the potential outcome assignment vector that corresponds to the dependency of x_3 on x_2 and x_2 on x_1 , as given by $\epsilon^{(3 \cdot 2 \cdot 1)} = \epsilon_2$.

Note that we do not introduce additional notation for the final dependency on the structural shock since this is by definition always the last element.

4.1.2 Potential Transmission Channels

Each potential outcomes assignment vector $\epsilon^{(j)}$ defines a thought experiment in which some chains experience a shock while others may not. The most basic thought experiment is the one in which all $\epsilon_i = \xi$, implying that all chains experience the same shock realisation as commonly investigated in impulse response analysis in macroeconomics. A conceptually different thought experiment is one in which $\epsilon_k = 0$, for some $1 \leq k \leq \eta(j)$, implying that some of the nested dependencies may experience a non-zero shock of size ξ , while others do not. Causality is then carried along a subset of all nested chains – equivalently, along a subset of paths through the graph – in other words, along a transmission channel. Throughout the paper we assume that a nested chain is either shut off ($\epsilon_k = 0$) or is active and together with all other active ones experiences the same realised shock size ($\epsilon_l = \xi$), as formalised in Assumption 3.

Assumption 3. The potential outcomes assignment vector $\epsilon^{(j)}$ consists of components $\epsilon_i \in \{0, \xi\}$ for all $1 \leq i \leq \eta(j)$.

We are now ready to define transmission channels in potential outcome notation.

Definition 4. Let $\epsilon^{(j)}$ be a potential outcomes assignment vector with ϵ_i satisfying Assumption 3. If $\epsilon_k = 0$ and $\epsilon_l = \xi$ for some k, l , then $\epsilon^{(j)}$ is a transmission channel.

Example 2 (continued). Consider the potential outcomes assignment vector $\epsilon^{(3)}$ for the non-recursive case displayed in Figure 5. If $\epsilon^{(3)} = (0, 1, 0, 0)$ implying $\epsilon^{(3 \cdot 2 \cdot 1)} = 1$, then only the second nested chain experiences a shock. This chain is shown in Figure 5 panel (c) and corresponds to a transmission channel in which the shock changes x_1 which in turn changes x_2 which finally changes x_3 . If $\epsilon^{(3)} = (0, 1, 1, 0)$, then we obtain the indirect transmission channel which corresponds to the combination of the second and third transmission channel shown in Figure 5 panels (c) and (d) respectively.

4.1.3 Causal Effects

The causal effect of a potential outcomes assignment vector measures the effect of a thought experiment by comparing it to a baseline. Under Assumption 3, a natural

baseline is $\epsilon_i = 0$ for all $i = 1, \dots, \eta(j)$ such that no chain experiences a shock. If $\epsilon^{(j)}$ is a transmission channel according to Definition 4, then the transmission effect compares the reaction of x_j under the thought experiment, $x_j^*(\epsilon^{(j)})$, to the reaction of x_j under the baseline, $x_j^*(\mathbf{0})$. This is the causal effect of $\epsilon^{(j)}$ on x_j .

Definition 5. The causal effect of the structural shock ϵ_i on the variable of interest x_j is given by

$$\mathcal{C}_{\epsilon_i, x_j}(\epsilon^{(j)}) = \mathbb{E}[x_j^*(\epsilon^{(j)}) - x_j^*(\mathbf{0})],$$

where $\epsilon^{(j)}$ is a potential outcomes assignment vector and $\mathbf{0}$ is a conformable vector of zeros. If $\epsilon^{(j)}$ is a transmission channel according to Definition 4, then $\mathcal{C}_{\epsilon_i, x_j}(\epsilon^{(j)})$ is the transmission effect of that transmission channel.

Example 2 (continued). Let $\epsilon^{(3)} = (e_1, e_2, e_3, e_4)$. Then

$$\begin{aligned} \mathbb{E}[x_3^*(\epsilon^{(3)})] &= B_{3,1} \mathbb{E}[x_1^*(\epsilon^{(3 \cdot 1)})] + B_{3,2} \mathbb{E}[x_2^*(\epsilon^{(3 \cdot 2)})] + \Omega_{3,1} e_4 \\ &= B_{3,1} \Omega_{1,1} e_1 + B_{3,2} B_{2,1} \mathbb{E}[x_1^*(\epsilon^{(3 \cdot 2 \cdot 1)})] + B_{3,2} \Omega_{2,1} e_3 + \Omega_{3,1} e_4 \\ &= B_{3,1} \Omega_{1,1} e_1 + B_{3,2} B_{2,1} \Omega_{1,1} e_2 + B_{3,2} \Omega_{2,1} e_3 + \Omega_{3,1} e_4 \end{aligned}$$

The transmission effect of the indirect transmission channel, $\epsilon^{(3)} = (0, 1, 1, 0)$ is therefore $\mathcal{C}_{\epsilon_i, x_j}(\epsilon^{(3)}) = B_{3,2}(B_{2,1}\Omega_{1,1} + \Omega_{2,1}) = (\alpha_2\alpha_4)/((1 + \alpha_1^2)\eta)$, while the transmission effect of the direct transmission channel, $\epsilon^{(3)} = (1, 0, 0, 1)$, is given by $\mathcal{C}_{\epsilon_i, x_j}(\epsilon^{(3)}) = B_{3,1}\Omega_{1,1} + \Omega_{3,1} = (\alpha_3 + \alpha_1(1 - \eta))/((1 + \alpha_1^2)\eta)$.

4.1.4 Equivalence to the Graphical Framework

Finally, in Theorem 1, we show that transmission channels defined in Definitions 2 and 4, and transmission effects defined in Definitions 3 and 5 are equivalent.

Theorem 1. Assume \mathbf{y}_t is generated by model (7) and Assumptions 1 to 3 hold, such that \mathbf{y}_t can be equivalently represented in static form (9). Let $\mathcal{G}(\mathbf{B}, \boldsymbol{\Omega})$ be the graph induced by the model. Consider the effect from the structural shock ϵ_i to the variable of interest x_j , then we have the following equivalence:

- (i) Given a collection of paths $P_{\epsilon_i, x_j} \subseteq \mathcal{P}_{\epsilon_i, x_j}$, there exists a potential outcomes assignment vector $\epsilon^{(j)}$ such that $\mathcal{Q}_{\xi}(P_{\epsilon_i, x_j}) = \mathcal{C}_{\epsilon_i, x_j}(\epsilon^{(j)})$.
- (ii) Given a potential outcomes assignment vector $\epsilon^{(j)}$, there exists a collection of paths $P_{\epsilon_i, x_j} \subseteq \mathcal{P}_{\epsilon_i, x_j}$ such that $\mathcal{C}_{\epsilon_i, x_j}(\epsilon^{(j)}) = \mathcal{Q}_{\xi}(P_{\epsilon_i, x_j})$.

Example 2 (continued). Figure 5 makes use of the equivalence result between the graphical and the potential outcomes frameworks. Panels (c) through (e) show on top the path that is either shut-off ($\epsilon_i = 0$; gray edges) or active ($\epsilon_i = \xi$; black edges) with the potential outcomes underneath highlighting which element in the potential outcomes assignment vector $\epsilon^{(3)}$ corresponds to the path under consideration.

4.2 Properties of TCA

The previous section introduced potential outcomes and showed in Theorem 1 that the potential outcomes and graphical framework for TCA are equivalent. In this section, we continue with the potential outcomes framework and use its equivalence with the graphical framework to derive three main results. We focus throughout on the (transmission) effect of the structural shock ε_i on x_j .

4.2.1 Total Effects

First, since causal effects flow along paths in the associated graph $\mathcal{G}(\mathbf{B}, \mathbf{\Omega})$, intuitively, the total causal effect should be the effect along all paths connecting ε_i and x_j , $\mathcal{P}_{\varepsilon_i, x_j}$. Theorem 2 shows that this is the case.

Theorem 2. Let $\mathbf{1}_{\eta(j)}$ be a $\eta(j)$ dimensional vector of ones, $P_{\varepsilon_i, x_j}^{(1)}, \dots, P_{\varepsilon_i, x_j}^{(k)}$ be a partition of $\mathcal{P}_{\varepsilon_i, x_j}$ and $\mathbf{e}_1 \dots \mathbf{e}_k$ be $\eta(j)$ dimensional vectors in $\{0, \xi\}^{\eta(j)}$ such that $\sum_{m=1}^k \mathbf{e}_m = \xi \mathbf{1}_{\eta(j)}$. Then, under the same conditions as in Theorem 1,

- (i) $\mathcal{Q}_\xi(\mathcal{P}_{\varepsilon_i, x_j}) = \mathcal{C}_{\varepsilon_i, x_j}(\xi \mathbf{1}_{\eta(j)}) = \xi \Phi_{j,i}$
- (ii) $\sum_{m=1}^k \mathcal{Q}_\xi(P_{\varepsilon_i, x_j}^{(m)}) = \xi \Phi_{j,i}$
- (iii) $\sum_{m=1}^k \mathcal{C}_{\varepsilon_i, x_j}(\mathbf{e}_m) = \xi \Phi_{j,i}$.

Part (i) states that the total effect given by entry $\Phi_{j,i}$ in the impulse response matrix is equal to the total path-specific effect of the collection of all paths $\mathcal{Q}_1(\mathcal{P}_{\varepsilon_i, x_j})$, which is in turn equal to the causal effect of the potential outcomes assignment vector $\epsilon^{(j)} = \mathbf{1}_{\eta(j)}$ by Theorem 1. Multiplication by ξ simply accounts for the shock size. Part (ii) states that the total path-specific effect of each set in the partition $P_{\varepsilon_i, x_j}^{(1)}, \dots, P_{\varepsilon_i, x_j}^{(k)}$ of $\mathcal{P}_{\varepsilon_i, x_j}$ decomposes the total effect. Thus, since each set $P_{\varepsilon_i, x_j}^{(i)}$ in the partition is a transmission channel by Definition 2, disjoint transmission channels decompose the total effect. Part (iii) implies that the same statement can be made for a set of potential outcomes assignment vectors $\mathbf{e}_1 \dots \mathbf{e}_k$ such that

$\sum_{m=1}^k e_m = \xi \mathbf{1}_{\eta(j)}$, which is the potential outcomes equivalent to the partition $P_{\varepsilon_i, x_j}^{(1)}, \dots, P_{\varepsilon_i, x_j}^{(k)}$.

4.2.2 IRF Sufficiency

While Theorem 2 shows that total effects are decomposed by non-overlapping transmission channels, it says nothing about how the transmission effects and can be obtained. This is the subject of Theorem 3.

Theorem 3. Let $\tilde{\Phi}$ be the impulse responses obtained using a Cholesky identification scheme following the ordering in \mathbf{T} . Then, under the same conditions as in Theorem 1, for some function $f : \mathbb{R}^{hK \times hK} \times \mathbb{R}^{hK \times hK} \rightarrow \mathbb{R}$, and for all x_r, x_s, x_j and ε_i with $r < s$,

- (i) $Q_1(\mathcal{P}_{x_r, x_s}) = \tilde{\Phi}_{s,r} \tilde{\Phi}_{r,r}^{-1}$
- (ii) $Q_\xi(P_{\varepsilon_i, x_j}) = f(\Phi, \tilde{\Phi})$.

Theorem 3 shows that the transmission effect of any transmission channel is a combination of the two impulse response matrices Φ and $\tilde{\Phi}$; thus, IRFs are sufficient statistics for the calculation of transmission effects. This extends known sufficiency results of IRFs for FEVDs (Kilian & Lütkepohl, 2017), policy counterfactual analysis (McKay & Wolf, 2023), and the analysis of policy optimality (Barnichon & Mesters, 2023). Note that although the sufficiency result makes use of a Cholesky identification scheme, the Cholesky scheme is not used to identify a structural shock; it is simply a computational tool. Only the impulse response matrix Φ is structural, while the matrix $\tilde{\Phi}$ contains orthogonalised impulse responses – they are orthogonalised with respect to the transmission matrix \mathbf{T} rather than a structural ordering.

The Cholesky impulse response matrix $\tilde{\Phi}$ used to compute transmission effects is sensitive to the ordering in \mathbf{T} ; however, the transformation f in Theorem 3 does not always make use of all columns in $\tilde{\Phi}$. In cases in which f only makes use of some columns of $\tilde{\Phi}$, results by Christiano et al. (1999) imply that only a partial variable ordering is needed. More precisely, if f makes use of the columns k_1, \dots, k_m then variables ordered between x_{k_i} ($1 \leq i < m$) and x_{k_j} ($i < j \leq m$) can be reordered, so can variables ordered before x_{k_1} or after x_{k_m} .

Example 2 (continued). Consider the transmission effect of the indirect channel for the non-recursive case displayed in Figure 5. This effect can be computed in two stages. In the first stage the effect follows all paths from the demand shock

to inflation and is given by the total effect α_2/η of the demand shock on inflation; hence a structural impulse response from Φ . In the second stage, the effect is carried further from inflation to interest rates and is given by $\alpha_4/(1 + \alpha_1^2)$; hence a Cholesky impulse response from $\tilde{\Phi}$ obtained following the ordering in $\mathbf{T} = \mathbf{I}$. Multiplying both IRFs results in the indirect effect in equation (6).

4.2.3 Identification Requirements

As the final step in our theoretical development, Theorem 4 shows that TCA only requires the shock of interest to be identified.

Theorem 4. Under the same conditions as in Theorem 1, transmission effects can be obtained if the i th column of the impulse response matrix, $\Phi_{\cdot,i}$, is known.

TCA provides additional insights into what drives equilibrium dynamics due to a structural shock ε_i . This implies that TCA only requires the identification of ε_i , the structural intervention under investigation. This stands in contrast to counterfactual policy analysis (e.g. McKay and Wolf (2023) or Sims and Zha (2006)), where in addition to ε_i further identified shocks are needed to mimic the counterfactual policy rule in a different dynamic equilibrium.

Theorem 3 and 4 together imply that TCA is feasible whenever standard macroeconomic analysis of total dynamic causal effects is feasible. In addition, the theoretical properties established provide guidance for the practical computation of transmission effects either by aggregating path effects, or by calculating the relevant impulse responses. While both approaches are valid, their computational efficiency will depend on the specific application. Appendix C goes into more details about the computational aspects and proposes an algorithm that exploits the established properties to yield a computationally efficient procedure.

5 Empirical Applications

In this section we demonstrate the versatility of TCA in gaining deeper insights beyond total impulse responses in a variety of settings. Section 5.1 considers monetary policy effects estimated using SVARs to demonstrate how TCA can be used to decompose monetary policy effects into contemporaneous and forward guidance effects. Section 5.2 applies TCA to government spending within a local projections (LP) framework to decompose the total effect of a government spending news shock into implementation and anticipation effects. Finally, Section 5.3 shows how

TCA can be used to decompose total impulse responses obtained from linearised DSGE models such as the prototypical Smets and Wouters (2007) model. Further details regarding data are provided in Appendix D, while all algorithms used for the computation of the transmission effects are implemented in the Julia package `TransmissionChannelAnalysis.jl`.³

5.1 Forward Guidance of Monetary Policy

We use TCA to decompose the effects of monetary policy shocks into contemporaneous effects, related to a direct change in the interest rate, and effects that are not linked to direct changes of the main policy instrument, such as forward guidance. McKay and Wolf (2023) argue that the Romer and Romer (2004, henceforth RR) shock series measures predominantly direct implementation effects of monetary policy, while the Gertler and Karadi (2015, henceforth GK) shock series rather capture the non-contemporaneous components of monetary policy such as forward guidance. TCA provides a framework to quantify and assess this hypothesis by decomposing the total impulse responses to either monetary policy shock into direct implementation and non-contemporaneous effects. To conduct TCA, we estimate an SVAR(4) in the federal funds rate i_t , the output gap x_t , inflation π_t and commodity prices p_t , and identify the monetary policy shock using either RR or GK as an internal instrument (Plagborg-Møller & Wolf, 2021).⁴

We define the direct implementation channel of monetary policy as the effect of a monetary policy shock going contemporaneously through an adjustment in the federal funds rate. The non-contemporaneous effect is then defined as the complement; the effect of the monetary policy shock not going through a contemporaneous adjustment in the federal funds rate. Since the federal funds rate is implicitly held constant on impact, the non-contemporaneous effect captures forward guidance effects.⁵

To correctly quantify the direct implementation channel, the federal funds rate should be ordered first in the transmission matrix. It follows from our theory that the transmission effects only depend on the structural impulse response of the federal funds rate, plus the reduced form responses from the federal funds rate to

³The package is available on GitHub: <https://github.com/enweg/TransmissionChannelAnalysis.jl>. Replication code for the empirical applications considered in this section is also available on GitHub: <https://github.com/enweg/tca-replication-material>.

⁴All data was obtained from the replication package of McKay and Wolf (2023).

⁵Note that other effects might also be captured. We leave a more thorough identification of forward guidance effects through a more precise definition of forward guidance channels to future research.

the variable of interest. Since these are invariant to the ordering of the remaining variables, any transmission matrix ordering the federal funds rate first results in the same transmission effects.

Figure 6 shows the total, direct implementation, and non-contemporaneous effects of the RR (top) and GK (bottom) shock, all normalised to a 25bp contemporaneous increase in the federal funds rate.⁶ The total effect is depicted as a scatter-line in black, while the direct implementation and non-contemporaneous effects are depicted as stacked bars in blue and yellow, respectively. The GK shock triggers dynamics in the federal funds rate and inflation that are clearly distinct from the dynamics induced by the RR shock. Additionally, the majority of the GK induced reactions are explained by non-contemporaneous effects, while only a small part of the reactions to an RR shock can be explained by non-contemporaneous effects. Thus, the results quantitatively confirm the qualitative discussion in McKay and Wolf (2023). The RR shock series measures mostly contemporaneous effects of monetary policy, while the GK shock series identifies non-contemporaneous components of monetary policy that are likely linked to forward guidance.

5.2 Anticipation Effects of Government Spending

In the previous section we defined the direct implementation channel of monetary policy as the effect of a policy that only goes through a contemporaneous change in the federal funds rate. In this section we build on this idea to specify a channel capturing the anticipation effects of government spending news shocks. The analysis is motivated by Ramey (2011, 2016a) and Ramey and Zubairy (2018) who argue that many series of identified government spending shocks, such as the war dates series (Ramey & Shapiro, 1998), do not correctly capture important anticipation effects. Since their proposed series captures news about government military spending, we define the anticipation channel as the effect of the news shock that is not driven by the response of government military spending up to horizon H .

In line with the original papers, we treat the news measure to be a direct measure of the shock, and thus include it as a variable directly. Given the definition

⁶Note that the scale of the impulse responses is determined by the chosen normalisation procedure, which makes a direct comparison in terms of absolute effects of the RR and GK shocks (on inflation) difficult. However, relative decompositions into transmission channels and qualitative conclusions about the shapes of the IRFs can be compared, since they are invariant to the chosen normalisation.

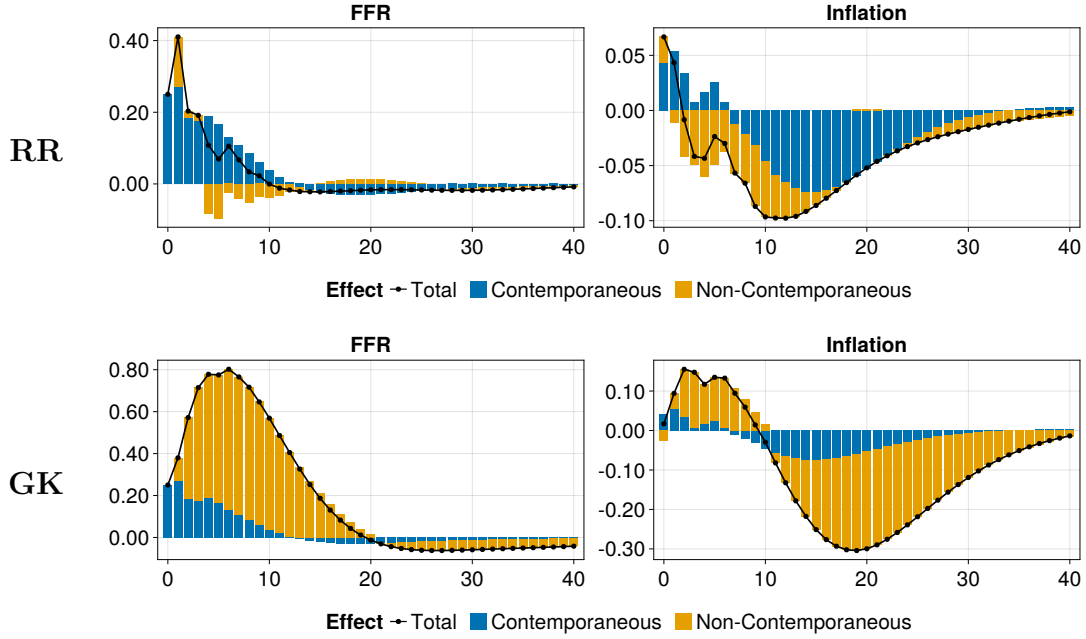


Figure 6: Decomposition of the total effect of an RR (top) and GK (bottom) identified monetary policy shock into a direct implementation and non-contemporaneous channel.

of the anticipation channel, government military spending should be ordered after the news series in the transmission matrix. Since all involved impulse responses are invariant to the ordering of the remaining variables, all transmission matrices which order the news variable first and government military spending second result in the same anticipation effects.

We estimate impulse responses using local projections. This involves estimating the following regression

$$y_{i,t+h} = \alpha^h + \beta_i^h \text{news}_t + \sum_{l=1}^4 \mathbf{y}'_{t-l} \psi_{i,l}^h + \varepsilon_{i,t}^h,$$

where $\mathbf{y}_t = (\text{news}_t, \text{mil}_t, \text{gov}_t, \text{gdp}_t)$, news_t is the news measure, mil_t government military spending, gov_t total government spending, and gdp_t is GDP, all expressed in real terms and as percent of real potential GDP. Then, β_i^h measures the impulse response of a news shock of one percent of real potential GDP on $y_{i,t+h} = x_{i+4h}$. To estimate transmission channels we need additional, reduced-form impulse responses. These are estimated using local projections of the form

$$y_{i,t+h} = \tilde{\alpha}^h + \tilde{\beta}_i^h \text{news}_t + \tilde{\gamma}_i^h \text{mil}_t + \sum_{l=1}^4 \mathbf{y}'_{t-l} \tilde{\psi}_{i,l}^h + \tilde{\varepsilon}_{i,t}^h,$$

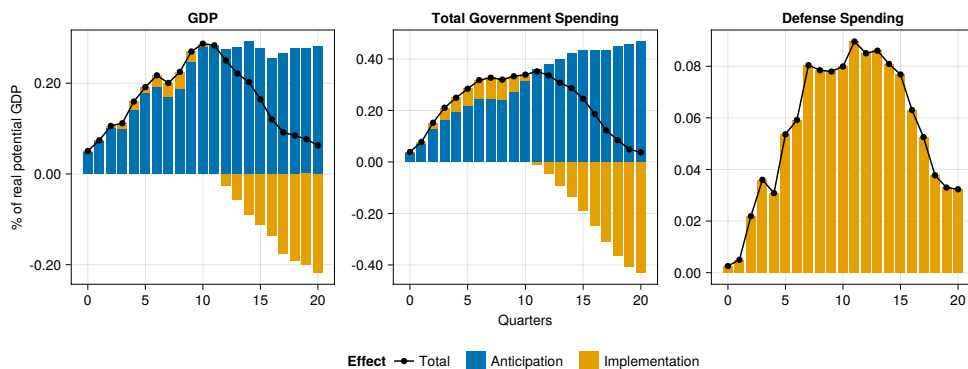


Figure 7: Decomposition of the total effect of a defense-news shock of one percent of potential GDP into an anticipation and implementation channel.

where $\tilde{\gamma}_i^h$ measures the Cholesky impulse response of a government military spending shock on $y_{i,t+h} = x_{i+4h}$, following the ordering defined in the transmission matrix. The anticipation and implementation effects that decompose the total impulse responses of a government spending news shock can then be computed using the algorithms of Appendix C.

Figure 7 shows the total, implementation, and anticipation effects of the government spending news shock on GDP, total government spending, and government military spending. The total effect is shown as a black scatter-line with the anticipation and implementation effect shown as stacked bars in blue and yellow respectively. By construction of the anticipation channel, government military spending is completely driven by implementation effects. GDP and total government spending, on the other hand, are largely driven by anticipation effects, with implementation effects remaining negligible for the first ten quarters and for the first three quarters for GDP and total government spending respectively. Thus, in line with Ramey (2011), reactions of GDP and, to a lesser extent, the reaction of total government spending seem largely driven by anticipation effects. Finally, note that anticipation and implementation effects do not return to zero even twenty periods after the shock. Instead, anticipation and implementation effects start to offset each other; a pattern that is hidden in total impulse responses but that becomes apparent when using TCA.

5.3 The Role of Inflation Expectations in DSGEs

In the previous sections we have studied transmission channels using time series models typically used in empirical macroeconomics. However, TCA can also be applied in other dynamic models often used in macroeconomic analysis, such as

DSGEs. Since DSGE models consist of many interrelated equilibrium equations, TCA may provide important insights into the exact mechanisms behind total dynamic effects.

We analyse the role of inflation expectations in the transmission of monetary policy shocks (i.e. unexpected changes in the policy rate) using the linearised Smets and Wouters (2007) model.⁷ This model formulates the dynamic relationship of the endogenous variables $r_t, \pi_t^e, w_t, c_t, i_t, y_t$, and π_t , where r_t is the policy rate, π_t^e are rational expectations of inflation, w_t is wage growth, c_t is consumption growth, i_t is investment growth, y_t is output growth, and π_t is realised inflation. TCA requires to re-formulate the linearised DSGE in SVARMA form. To do so we use the method of Morris (2016).

Given the set of endogenous variables, specifically the inclusion of inflation expectations π_t^e , the total dynamic effect of a monetary policy shock on inflation can be decomposed into three mutually exclusive transmission channels. First, a pure interest rate channel can be defined as the effect not going through any of $(\pi_t^e, w_t, c_t, i_t, y_t)$ in any period, representing the direct effect of the shock on inflation and the indirect effect of the shock on inflation carried by responses of interest rates. For a logical definition of this channel, we need r_t to be ordered first in the transmission matrix. Second, an expectations channel can be defined as the effect through expectations π_t^e but not through any other economic variables, (w_t, c_t, i_t, y_t) , in any period, requiring π_t^e to be ordered second. Third, an output and wage channel can be defined as the effect through any of (w_t, c_t, i_t, y_t) in at least one period, implying that (w_t, c_t, i_t, y_t) must be ordered after r_t and π_t^e , and before π_t , but the ordering within the group (w_t, c_t, i_t, y_t) does not matter.

Given the choice of transmission matrix and the defined transmission channels, the transmission effects can be obtained by applying the algorithms of Appendix C. Figure 8 shows the humped-shaped total effect of a contractionary monetary policy shock on inflation as a black scatter-line. The effect of the pure interest rate channel, the effect of the expectations channel, and the effect of the output and wage channel are respectively shown in blue, red, and yellow bars. The channels perfectly decompose the total effect implying that their sum equals the total effect.

The expectations channel is the most relevant channel at all horizons. After a contractionary monetary policy shock, inflation expectations decrease leading to a decrease in realised inflation. Without this channel, i.e. without the red bars, the monetary policy shock would show an initial increase in inflation. Thus,

⁷Replication files including the standard parameterisation of the Smets and Wouters (2007) model were obtained from Pfeifer (2024).

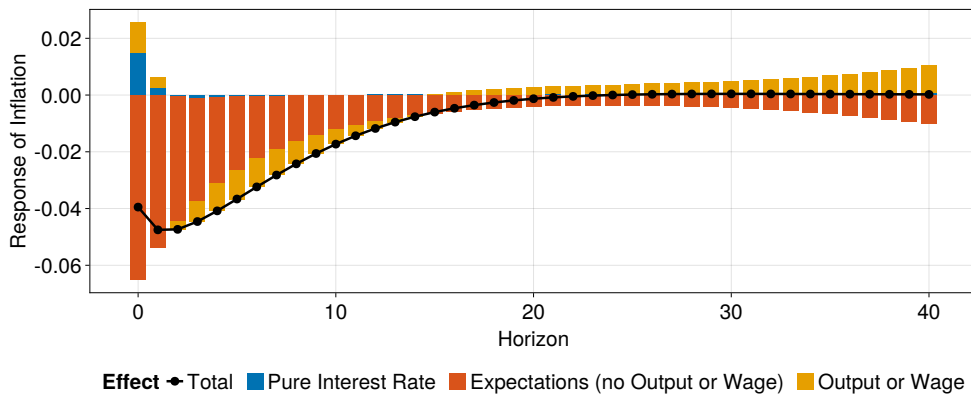


Figure 8: Decomposition of the total effect of a contractionary monetary policy shock, within the Smets and Wouters (2007) model, into a pure interest rate, expectations, and output-wage channel.

empirically identified monetary policy shocks showing the common price-puzzle may correspond to monetary policy shocks which fail to accurately capture the expectations channel.

The pure interest rate channel and the output and wage channel are much less important for the transmission of the monetary policy shock to inflation. Both show an initial positive effect, but the effect dies out after around two periods for the pure interest rate channel, while it turns negative for the output and wage channel. More importantly, the effect through the output and wage channel never returns to zero, nor does the expectations effect. Instead, the effect through the output and wage channel, and through the expectations channel start to perfectly offset each other after about twenty-two periods. Thus, while the pure interest rate channel plays no role in bringing the economy back to equilibrium, the interaction between the expectations, and the output and wage channel is key in bringing the economy back to equilibrium; a fact hidden in dynamic total effects which always allow for such interactions.

6 Conclusion

We develop a new coherent framework for transmission channel analysis for a large class of dynamic models by connecting them to a graphical representation. Within the graphical representation, transmission channels are defined as paths connecting the shock of interest to the outcome variable; transmission effects are the effects flowing along these paths. We show that this graphical representation is equivalent to a potential outcomes representation which we use to prove that

impulse responses are sufficient for the computation of all transmission effects.

Current methods to analyse transmission channels are purely based on qualitative inspections of various impulse responses. These qualitative assessments cannot be used to quantitatively compare the importance of various transmission channels. Our framework opens up the way for a formal quantitative analysis of transmission channels, therefore extending the toolbox of the empirical macroeconomic researcher. Of particular relevance for applied work is our result that TCA does not require any additional identification requirements beyond the identification of the structural shock of interest.

A crucial component of TCA is a precise definition of the transmission channel of interest. We showed how this can be formalised through the transmission matrix which defines the *ceteris paribus* ordering of the variables in equilibrium; this ordering is entirely defined by the research question. We also show that under some cases, a partial ordering is sufficient. This is also the case in our empirical applications, in which we show how TCA can shed a quantitative light on the channels through which policy operates in a variety of macroeconomic settings.

While our proposed framework is applicable to a large set of commonly used dynamic macroeconomic models, including SVARs, DSGEs, and local projections, it is currently not applicable to general state space models, which are used to model dynamics via a system of latent variables. While some state space representations, such as those used for DSGE models, can be rewritten into SVARMA form, this rewriting cannot accommodate all such models; in particular, one cannot apply our framework directly to dynamic factor models. In state space models, transmission channels and effects can still be defined in an equivalent way using either the graphical or the potential outcomes representation. However, this definition comes with statistical identification problems that are beyond the scope of this paper. We therefore leave this extension for future research.

Our proposed framework relies on linearity of the dynamic model and is thus inherently subject to potential shortcomings of linear models. This might be considered a limitation as some evidence points to nonlinear effects of policies. For example, effects of monetary expansions and contractions are clearly distinct (Angrist et al., 2018; Cover, 1992; Tenreyro & Thwaites, 2016). This difference may well be driven by the difference in the transmission of an expansionary and a contractionary shock. Under the current setup, TCA cannot make a difference in expansionary and contractionary shocks – it simply analyses the average transmission effects unconditional of the sign. However, most of macroeconomic analysis

still relies on linear dynamic models, and TCA is applicable in a very wide class of these. TCA in its current form can therefore already complement the vast majority of empirical macroeconomic analyses. In addition, extending TCA to nonlinear models, particularly when allowing for interaction effects, requires a complete re-think of how to define transmission channels. This is another exciting avenue for future research.

Acknowledgements. The last author was financially supported by the Dutch Research Council (NWO) under grant number VI.Vidi.211.032. Previous versions of this paper were presented at the Maastricht MILE seminar, the European Seminar on Bayesian Econometrics 2023, and the NESG 2023 conference. We gratefully acknowledge comments by participants at these seminars and conferences. Remaining errors are our own.

References

- Angrist, J. D., Jordà, Ò., & Kuersteiner, G. M. (2018). Semiparametric estimates of monetary policy effects: String theory revisited. *Journal of Business & Economic Statistics*, *36*(3), 371–387. <https://doi.org/10.1080/07350015.2016.1204919>
- Arias, J. E., Rubio-Ramírez, J. F., & Waggoner, D. F. (2018). Inference based on structural vector autoregressions identified with sign and zero restrictions: Theory and applications. *Econometrica*, *86*(2), 685–720. <https://doi.org/10.3982/ecta14468>
- Barnichon, R., & Mesters, G. (2020). Identifying modern macro equations with old shocks. *The Quarterly Journal of Economics*, *135*(4), 2255–2298. <https://doi.org/10.1093/qje/qjaa022>
- Barnichon, R., & Mesters, G. (2023). A sufficient statistics approach for macro policy. *American Economic Review*, *113*(11), 2809–2845. <https://doi.org/10.1257/aer.20220581>
- Chan, K. C. G., Imai, K., Yam, S. C. P., & Zhang, Z. (2016). Efficient nonparametric estimation of causal mediation effects. <https://doi.org/10.48550/arxiv.1601.03501>
- Chiswell, I., & Hodges, W. (2007). *Mathematical logic*. Oxford University Press.
- Christiano, L. J., Eichenbaum, M., & Evans, C. L. (1999). Monetary policy shocks: What have we learned and to what end? In *Handbook of Macroeconomics* (pp. 65–148, Vol. 1A).

- Cloyne, J., Jordà, Ò., & Taylor, A. M. (2023). *State-dependent local projections: Understanding impulse response heterogeneity* (Working Paper No. 30971). National Bureau of Economic Research.
- Cover, J. P. (1992). Asymmetric effects of positive and negative money-supply shocks. *The Quarterly Journal of Economics*, *107*(4), 1261–1282. <https://doi.org/10.2307/2118388>
- Daniel, R. M., De Stavola, B. L., Cousens, S. N., & Vansteelandt, S. (2015). Causal mediation analysis with multiple mediators. *Biometrics*, *71*(1), 1–14. <https://doi.org/10.1111/biom.12248>
- Fernández-Villaverde, J., Rubio-Ramírez, J. F., Sargent, T. J., & Watson, M. W. (2007). ABCs (and Ds) of understanding VARs. *American Economic Review*, *97*(3), 1021–1026. <https://doi.org/10.1257/aer.97.3.1021>
- Galí, J. (2015). *Monetary policy, inflation, and the business cycle: An introduction to the new Keynesian framework and its applications* (2nd ed.). Princeton University Press.
- Gertler, M., & Karadi, P. (2015). Monetary policy surprises, credit costs, and economic activity. *American Economic Journal: Macroeconomics*, *7*(1), 44–76. <https://doi.org/10.1257/mac.20130329>
- Hayes, A. F. (2018). *Introduction to mediation, moderation, and conditional process analysis: A regression-based approach* (2nd ed.). Guilford Press.
- Imai, K., Keele, L., & Yamamoto, T. (2010). Identification, inference and sensitivity analysis for causal mediation effects. *Statistical Science*, *25*(1), 51–71. <https://doi.org/10.1214/10-sts321>
- Jordà, Ò. (2005). Estimation and inference of impulse responses by local projections. *American Economic Review*, *95*(1), 161–182. <https://doi.org/10.1257/0002828053828518>
- Kilian, L., & Lewis, L. T. (2011). Does the fed respond to oil price shocks? *The Economic Journal*, *121*(555), 1047–1072. <https://doi.org/10.1111/j.1468-0297.2011.02437.x>
- Kilian, L., & Lütkepohl, H. (2017). *Structural vector autoregressive analysis*. Cambridge University Press. <https://doi.org/10.1017/9781108164818>
- McKay, A., & Wolf, C. K. (2023). What can time-series regressions tell us about policy counterfactuals? *Econometrica*, *91*(5), 1695–1725. <https://doi.org/10.3982/ecta21045>
- Mertens, K., & Ravn, M. O. (2013). The dynamic effects of personal and corporate income tax changes in the united states. *American Economic Review*, *103*(4), 1212–1247. <https://doi.org/10.1257/aer.103.4.1212>

- Morris, S. D. (2016). VARMA representation of DSGE models. *Economics Letters*, 138, 30–33. <https://doi.org/10.1016/j.econlet.2015.11.027>
- Nakamura, E., & Steinsson, J. (2018). Identification in macroeconomics. *Journal of Economic Perspectives*, 32(3), 59–86. <https://doi.org/10.1257/jep.32.3.59>
- Pearl, J. (2009). *Causality: Models, reasoning, and inference* (2nd ed.). Cambridge University Press. <https://doi.org/10.1017/cbo9780511803161>
- Pearl, J. (2012). The causal mediation formula – a guide to the assessment of pathways and mechanisms. *Prevention Science*, 13, 426–436. <https://doi.org/10.1007/s11121-011-0270-1>
- Pfeifer, J. (2024, March). *DSGE_mod: A collection of dynare models*. <https://doi.org/10.5281/zenodo.10810290>
- Plagborg-Møller, M., & Wolf, C. K. (2021). Local projections and VARs estimate the same impulse responses. *Econometrica*, 89(2), 955–980. <https://doi.org/10.3982/ecta17813>
- Poskitt, D. (1992). Identification of echelon canonical forms for vector linear processes using least squares. *The Annals of Statistics*, 20, 195–215.
- Rambachan, A., & Shephard, N. (2021). When do common time series estimands have nonparametric causal meaning?
- Ramey, V. A. (2011). Identifying government spending shocks: It’s all in the timing. *The Quarterly Journal of Economics*, 126(1), 1–50. <https://doi.org/10.1093/qje/qjq008>
- Ramey, V. A. (2016a). Defense news shocks, 1889 - 2015: Estimates based on news sources. *Unpublished paper, University of California, San Diego*.
- Ramey, V. A. (2016b). Macroeconomic shocks and their propagation. In *Handbook of macroeconomics* (pp. 71–162, Vol. 2).
- Ramey, V. A., & Shapiro, M. D. (1998). Costly capital reallocation and the effects of government spending. *Carnegie-Rochester Conference Series on Public Policy*, 48, 145–194. [https://doi.org/10.1016/s0167-2231\(98\)00020-7](https://doi.org/10.1016/s0167-2231(98)00020-7)
- Ramey, V. A., & Zubairy, S. (2018). Government spending multipliers in good times and in bad: Evidence from US historical data. *Journal of Political Economy*, 126(2), 850–901. <https://doi.org/10.1086/696277>
- Rautenberg, W. (2010). *A concise introduction to mathematical logic* (3rd ed.). Springer. <https://doi.org/10.1007/978-1-4419-1221-3>
- Ravenna, F. (2007). Vector autoregressions and reduced form representations of DSGE models. *Journal of Monetary Economics*, 54(7), 2048–2064. <https://doi.org/10.1016/j.jmoneco.2006.09.002>

- Romer, C. D., & Romer, D. H. (2004). A new measure of monetary shocks: Derivation and implications. *American Economic Review*, 94(4), 1055–1084. <https://doi.org/10.1257/0002828042002651>
- Sims, C. A., & Zha, T. (2006). Does monetary policy generate recessions? *Macroeconomic Dynamics*, 10(2), 231–272. <https://doi.org/10.1017/s136510050605019x>
- Smets, F., & Wouters, R. (2007). Shocks and frictions in US business cycles: A bayesian DSGE approach. *American Economic Review*, 97(3), 586–606. <https://doi.org/10.1257/aer.97.3.586>
- Tenreyro, S., & Thwaites, G. (2016). Pushing on a string: US monetary policy is less powerful in recessions. *American Economic Journal: Macroeconomics*, 8(4), 43–74. <https://doi.org/10.1257/mac.20150016>
- Wieland, J. F., & Yang, M.-J. (2020). Financial dampening. *Journal of Money, Credit and Banking*, 52(1), 79–113. <https://doi.org/10.1111/jmcb.12681>

Appendix A From structural VARMA to Systems Form

In this appendix, we provide details how the lower-triangular form of the structural VARMA given by

$$\mathbf{L}\mathbf{y}_t^* = \sum_{i=1}^{\ell} \mathbf{Q}'\mathbf{A}_i^*\mathbf{y}_{t-i}^* + \sum_{j=1}^q \mathbf{Q}'\boldsymbol{\Psi}_j\boldsymbol{\varepsilon}_{t-j} + \mathbf{Q}'\boldsymbol{\varepsilon}_t, \quad (\text{A.1})$$

as presented in equation (8) can be re-written into the general systems form

$$\mathbf{x} = \mathbf{B}\mathbf{x} + \boldsymbol{\Omega}\boldsymbol{\varepsilon}, \quad (\text{A.2})$$

as presented in equation (9).

Let h be the fixed finite horizon of the transmission channels under consideration. Equation (A.1) for time points $t, \dots, t+h$ can then be represented as the system of equations

$$\begin{cases} \mathbf{L}\mathbf{y}_t^* = \sum_{i=1}^{\ell} \mathbf{Q}'\mathbf{A}_i^*\mathbf{y}_{t-i}^* + \sum_{j=1}^q \mathbf{Q}'\boldsymbol{\Psi}_j\boldsymbol{\varepsilon}_{t-j} + \mathbf{Q}'\boldsymbol{\varepsilon}_t \\ \vdots \\ \mathbf{L}\mathbf{y}_{t+h}^* = \sum_{i=1}^{\ell} \mathbf{Q}'\mathbf{A}_i^*\mathbf{y}_{t+h-i}^* + \sum_{j=1}^q \mathbf{Q}'\boldsymbol{\Psi}_j\boldsymbol{\varepsilon}_{t+h-j} + \mathbf{Q}'\boldsymbol{\varepsilon}_{t+h}, \end{cases} \quad (\text{A.3})$$

which contains all information of the dynamic system up to horizon h . Multiplying all equations on the left-hand-side and right-hand-side by $\mathbf{D} = \text{diag}(\mathbf{L})^{-1}$, where

$\text{diag}(\mathbf{X})$ is a diagonal matrix containing the diagonal of \mathbf{X} , and moving $(\mathbf{I} - \mathbf{DL})\mathbf{y}_{t+i}^*$ to the right-hand-side in equations $i = 0, \dots, h$, we obtain

$$\begin{cases} \mathbf{y}_t^* = (\mathbf{I} - \mathbf{DL})\mathbf{y}_t^* + \sum_{i=1}^{\ell} \mathbf{DQ}'\mathbf{A}_i^*\mathbf{y}_{t-i}^* + \sum_{j=1}^q \mathbf{DQ}'\boldsymbol{\Psi}_j\boldsymbol{\varepsilon}_{t-j} + \mathbf{DQ}'\boldsymbol{\varepsilon}_t \\ \vdots \\ \mathbf{y}_{t+h}^* = (\mathbf{I} - \mathbf{DL})\mathbf{y}_{t+h}^* + \sum_{i=1}^{\ell} \mathbf{DQ}'\mathbf{A}_i^*\mathbf{y}_{t+h-i}^* + \sum_{j=1}^q \mathbf{DQ}'\boldsymbol{\Psi}_j\boldsymbol{\varepsilon}_{t+h-j} + \mathbf{DQ}'\boldsymbol{\varepsilon}_{t+h}. \end{cases} \quad (\text{A.4})$$

Given a shock in period t , then variables \mathbf{y}_{t-i}^* for $i > 0$ are unaffected by the shock, and thus do not play a role in the propagation of the shock. We may therefore ignore them by setting their corresponding coefficients equal to zero. System (A.4) then becomes

$$\begin{cases} \mathbf{y}_t^* = (\mathbf{I} - \mathbf{DL})\mathbf{y}_t^* + \mathbf{DQ}'\boldsymbol{\varepsilon}_t \\ \vdots \\ \mathbf{y}_{t+h}^* = (\mathbf{I} - \mathbf{DL})\mathbf{y}_{t+h}^* + \sum_{i=1}^{\min(h,p)} \mathbf{DQ}'\mathbf{A}_i^*\mathbf{y}_{t+h-i}^* + \sum_{j=1}^{\min(h,q)} \mathbf{DQ}'\boldsymbol{\Psi}_j\boldsymbol{\varepsilon}_{t+h-j} + \mathbf{DQ}'\boldsymbol{\varepsilon}_{t+h}. \end{cases} \quad (\text{A.5})$$

System (A.5) is then equivalent to the general form (A.2), with $\mathbf{x} = (\mathbf{y}_t^*, \dots, \mathbf{y}_{t+h}^*)'$, $\boldsymbol{\varepsilon} = (\boldsymbol{\varepsilon}'_t, \dots, \boldsymbol{\varepsilon}'_{t+h})'$, and

$$\mathbf{B} = \begin{bmatrix} \mathbf{I} - \mathbf{DL} & \mathbf{O} & \dots & \mathbf{O} \\ \mathbf{DQ}'\mathbf{A}_1^* & \mathbf{I} - \mathbf{DL} & \dots & \mathbf{O} \\ \vdots & \ddots & \ddots & \vdots \\ \mathbf{DQ}'\mathbf{A}_h^* & \dots & \mathbf{DQ}'\mathbf{A}_1^* & \mathbf{I} - \mathbf{DL} \end{bmatrix}, \quad \boldsymbol{\Omega} = \begin{bmatrix} \mathbf{DQ}' & \mathbf{O} & \dots & \mathbf{O} \\ \mathbf{DQ}'\boldsymbol{\Psi}_1 & \mathbf{DQ}' & \dots & \mathbf{O} \\ \vdots & \ddots & \ddots & \vdots \\ \mathbf{DQ}'\boldsymbol{\Psi}_h & \dots & \mathbf{DQ}'\boldsymbol{\Psi}_1 & \mathbf{DQ}' \end{bmatrix}, \quad (\text{A.6})$$

as given in equation (10) of Section 3.

Appendix B Proofs of Main Theorems

Section B.1 first introduces some notation and preliminary results based on Boolean algebra needed in the proofs of the main theorems. The proofs of Theorems 1 to 4 are then presented in Section B.2.

B.1 Boolean Algebra and Transmission Channels

Definition 2 defines transmission channels as a sub-collection of paths. In practice, it is more convenient to define transmission channels by verbal statements about which variables lie on the paths and which do not. Boolean algebra hereby plays an important role in translating verbal statements of transmission channels into sub-

collections of paths. In this section, we introduce the basics of Boolean algebra⁸ needed in the context of TCA. The main result of this section is Lemma 1 which provides an algebra for transmission channels and is key to proving Theorems 2, 3, and 4.

Let b be a Boolean formula that is true if and only if a path satisfies it, and false otherwise. We denote $\mathcal{P}_{u,v}$ the collection of all paths in $\mathcal{G}(\mathbf{B}, \mathbf{\Omega})$ from variable or shock u to variable v . Then $P_{u,v}(b) \subseteq \mathcal{P}_{u,v}$ represents the sub-collection of paths of $\mathcal{P}_{u,v}$ that satisfy the Boolean formula b . By Definition 2, $P_{u,v}(b)$ is a transmission channel as long as u is a shock and as long as at least one path is not satisfying the Boolean formula b .

A Boolean formula can consist of the following elements:

1. u : denotes that variable u must be on the paths.
2. $b' \wedge u$: denotes that the paths must satisfy the Boolean formula b' , and variable u must be on the paths.
3. $b' \wedge b''$: denotes that both Boolean formulas b' and b'' must be satisfied by the paths.
4. $b' \vee u$: denotes that the paths must either satisfy the boolean formula b' or u must be on the paths, or both.
5. $b' \vee b''$: denotes that the paths must either satisfy the boolean formula b' or b'' or both.
6. $\neg u$: denotes that variable u cannot be on the paths.
7. $\neg b'$: denotes that the Boolean formula b' cannot be satisfied by the paths.

In line with Definition 3, denote the total path-specific effect of the collection $P_{u,v}(b)$ by

$$\mathcal{Q}_\xi[P_{u,v}(b)] = \xi \sum_{p \in P_{u,v}(b)} \prod_{(k \rightarrow l) \in p} \omega_{kl},$$

where ξ is the shock size, and $\omega_{k,l}$ is the path coefficient of the edge going from node k to node l on path p .

Employing standard set theory arguments and Boolean algebra, several properties of the total path-specific effect can be demonstrated. These properties are collected in the next lemma.

⁸For a more in depth overview of Boolean algebra and mathematical logic see Chiswell and Hodges (2007) and Rautenberg (2010).

Lemma 1. Suppose \mathbf{y}_t is generated by model (7) and Assumptions 1 through 3 are satisfied. Let $\mathcal{G}(\mathbf{B}, \boldsymbol{\Omega})$ be the graph induced by model (9). Denote with $\mathcal{P}_{u,v}$ the set of all paths connecting variable or shock u to variable v in $\mathcal{G}(\mathbf{B}, \boldsymbol{\Omega})$ and by $P_{u,v}(b) \subseteq \mathcal{P}_{u,v}$ the subset of paths satisfying a Boolean formula b . Further, denote $\mathcal{Q}_\xi[P_{u,v}(b)]$ the total path-specific effect of the paths in $P_{u,v}(b)$. Then, the following properties hold:

(i) Let $b = x_k$. Then $\mathcal{Q}_\xi[P_{\varepsilon_i, x_j}(b)] = \mathcal{Q}_\xi[\mathcal{P}_{\varepsilon_i, x_k}] \mathcal{Q}_1[\mathcal{P}_{x_k, x_j}]$ with $k \neq j$.

(ii) Let $i_1 < i_2 < \dots < i_k$ and $i_k \neq j$. Let $b = \bigwedge_{m=1}^k x_{i_m}$. Then

$$\mathcal{Q}_\xi[P_{\varepsilon_i, x_j}(b)] = \mathcal{Q}_\xi[\mathcal{P}_{\varepsilon_i, x_{i_1}}] \mathcal{Q}_1[\mathcal{P}_{x_{i_1}, x_{i_2}}] \dots \mathcal{Q}_1[\mathcal{P}_{x_{i_k}, x_j}].$$

(iii) Let $P_{\varepsilon_i, x_j} \subset \mathcal{P}_{\varepsilon_i, x_j}$ and $P'_{\varepsilon_i, x_j} \subset \mathcal{P}_{\varepsilon_i, x_j}$ be two disjoint sets of paths. Then $\mathcal{Q}_\xi[P_{\varepsilon_i, x_j} \cup P'_{\varepsilon_i, x_j}] = \mathcal{Q}_\xi[P_{\varepsilon_i, x_j}] + \mathcal{Q}_\xi[P'_{\varepsilon_i, x_j}]$.

(iv) Let $P_{\varepsilon_i, x_j} \subset \mathcal{P}_{\varepsilon_i, x_j}$ and $P'_{\varepsilon_i, x_j} \subset \mathcal{P}_{\varepsilon_i, x_j}$. Then $\mathcal{Q}_\xi[P_{\varepsilon_i, x_j} \setminus P'_{\varepsilon_i, x_j}] = \mathcal{Q}_\xi[P_{\varepsilon_i, x_j}] - \mathcal{Q}_\xi[P_{\varepsilon_i, x_j} \cap P'_{\varepsilon_i, x_j}]$.

(v) Let b, b' be two Boolean formulas. Then $P_{\varepsilon_i, x_j}(b) \cap P_{\varepsilon_i, x_j}(b') = P_{\varepsilon_i, x_j}(b \wedge b')$.

(vi) Let b, b' be two Boolean formulas. Then $P_{\varepsilon_i, x_j}(b \vee b') = P_{\varepsilon_i, x_j}(b) \cup (P_{\varepsilon_i, x_j}(b') \setminus P_{\varepsilon_i, x_j}(b \wedge b'))$.

(vii) Let b, b' be two Boolean formulas. Then $P_{\varepsilon_i, x_j}(b \wedge \neg b') = P_{\varepsilon_i, x_j}(b) \setminus P_{\varepsilon_i, x_j}(b \wedge b')$.

(viii) Let $b = \neg x_k$. Then $\mathcal{Q}_\xi[P_{\varepsilon_i, x_j}(b)] = \mathcal{Q}_\xi[\mathcal{P}_{\varepsilon_i, x_j}] - \mathcal{Q}_\xi[P_{\varepsilon_i, x_j}(x_k)]$ with $i \neq j$.

Proof of Lemma 1(i). Each path $p \in P_{\varepsilon_i, x_j}(b)$ can be split into two parts: p_1 which goes from ε_i to x_k , and p_2 which goes from x_k to x_j . So we have $P_{\varepsilon_i, x_j}(b) = \mathcal{P}_{\varepsilon_i, x_k} \otimes \mathcal{P}_{x_k, x_j}$ where \otimes denotes the cross product of paths: For $p_1 \in \mathcal{P}_{\varepsilon_i, x_k}$ and $p_2 \in \mathcal{P}_{x_k, x_j}$, $p_1 \rightarrow p_2 \in \mathcal{P}_{\varepsilon_i, x_k} \otimes \mathcal{P}_{x_k, x_j}$. The total path specific effect can then be written as

$$\begin{aligned} \mathcal{Q}_\xi[P_{\varepsilon_i, x_j}(b)] &= \xi \sum_{p \in P_{\varepsilon_i, x_j}(b)} \prod_{(u \rightarrow v) \in p} \omega_{uv} \\ &= \xi \sum_{p_1 \in \mathcal{P}_{\varepsilon_i, x_k}} \sum_{p_2 \in \mathcal{P}_{x_k, x_j}} \left(\prod_{(u \rightarrow v) \in p_1} \omega_{uv} \right) \left(\prod_{(u \rightarrow v) \in p_2} \omega_{uv} \right) \\ &= \xi \sum_{p_1 \in \mathcal{P}_{\varepsilon_i, x_k}} \left\{ \prod_{(u \rightarrow v) \in p_1} \omega_{uv} \right\} \sum_{p_2 \in \mathcal{P}_{x_k, x_j}} \left\{ \prod_{(u \rightarrow v) \in p_2} \omega_{uv} \right\} \\ &= \mathcal{Q}_\xi[\mathcal{P}_{\varepsilon_i, x_k}] \mathcal{Q}_1[\mathcal{P}_{x_k, x_j}]. \quad \square \end{aligned}$$

Proof of Lemma 1(ii). We prove this by induction. We know from Lemma 1(i) that it holds for $k = 1$. Now suppose it holds for some k . We then need to show that it holds for $k + 1$. To do so, first define $b_k = \bigwedge_{m=1}^k x_{i_m}$ and $b_{k+1} = \bigwedge_{m=1}^{k+1} x_{i_m}$. Any path $p \in P_{\varepsilon_i, x_j}(b_{k+1})$ can then be split into three parts: $p_1 \in P_{\varepsilon_i, x_{i_k}}(b_k)$, $p_2 \in \mathcal{P}_{x_{i_k}, x_{i_{k+1}}}$, and $p_3 \in \mathcal{P}_{x_{i_{k+1}}, x_j}$. The following is then an extension of the proof to 1(i):

$$\begin{aligned}
\mathcal{Q}_\xi[P_{\varepsilon_i, x_j}(b_{k+1})] &= \xi \sum_{p \in P_{\varepsilon_i, x_j}(b_{k+1})} \prod_{(u \rightarrow v) \in p} \omega_{u,v} \\
&= \xi \sum_{p_1 \in P_{\varepsilon_i, x_{i_k}}(b_k)} \sum_{p_2 \in \mathcal{P}_{x_{i_k}, x_{i_{k+1}}}} \sum_{p_3 \in \mathcal{P}_{x_{i_{k+1}}, x_j}} \left(\prod_{(u \rightarrow v) \in p_1} \omega_{u,v} \right) \left(\prod_{(u \rightarrow v) \in p_2} \omega_{u,v} \right) \left(\prod_{(u \rightarrow v) \in p_3} \omega_{u,v} \right) \\
&= \xi \sum_{p_1 \in P_{\varepsilon_i, x_{i_k}}(b_k)} \left\{ \prod_{(u \rightarrow v) \in p_1} \omega_{u,v} \right\} \sum_{p_2 \in \mathcal{P}_{x_{i_k}, x_{i_{k+1}}}} \left\{ \prod_{(u \rightarrow v) \in p_2} \omega_{u,v} \right\} \sum_{p_3 \in \mathcal{P}_{x_{i_{k+1}}, x_j}} \left\{ \prod_{(u \rightarrow v) \in p_3} \omega_{u,v} \right\} \\
&= \mathcal{Q}_\xi[P_{\varepsilon_i, x_{i_k}}(b_k)] \mathcal{Q}_1[\mathcal{P}_{x_{i_k}, x_{i_{k+1}}}] \mathcal{Q}_1[\mathcal{P}_{x_{i_{k+1}}, x_j}].
\end{aligned}$$

By the induction hypothesis,

$$\mathcal{Q}_\xi[P_{\varepsilon_i, x_{i_k}}(b_k)] = \mathcal{Q}_\xi[P_{\varepsilon_i, x_{i_1}}] \mathcal{Q}_1[\mathcal{P}_{x_{i_1}, x_{i_2}}] \cdots \mathcal{Q}_1[\mathcal{P}_{x_{i_{k-1}}, x_{i_k}}].$$

Thus, the statement holds for $k + 1$. This implies that it holds for all $k \in \mathbb{N}$, concluding the proof. \square

Proof of Lemma 1(iii). Since for any $p \in P_{\varepsilon_i, x_j} \cup P'_{\varepsilon_i, x_j}$, we have $p \in P_{\varepsilon_i, x_j}$ or $p \in P'_{\varepsilon_i, x_j}$ but never in both, we can write

$$\begin{aligned}
\mathcal{Q}_\xi[P_{\varepsilon_i, x_j} \cup P'_{\varepsilon_i, x_j}] &= \xi \sum_{p \in P_{\varepsilon_i, x_j} \cup P'_{\varepsilon_i, x_j}} \prod_{(u \rightarrow v) \in p} \omega_{u,v} \\
&= \xi \sum_{p \in P_{\varepsilon_i, x_j}} \prod_{(u \rightarrow v) \in p} \omega_{u,v} + \xi \sum_{p \in P'_{\varepsilon_i, x_j}} \prod_{(u \rightarrow v) \in p} \omega_{u,v} \\
&= \mathcal{Q}_\xi[P_{\varepsilon_i, x_j}] + \mathcal{Q}_\xi[P'_{\varepsilon_i, x_j}]. \quad \square
\end{aligned}$$

Proof of Lemma 1(iv). Make the following two observations:

1. $P_{\varepsilon_i, x_j} \setminus P'_{\varepsilon_i, x_j}$ and $P_{\varepsilon_i, x_j} \cap P'_{\varepsilon_i, x_j}$ are disjoint.
2. $P_{\varepsilon_i, x_j} \setminus P'_{\varepsilon_i, x_j} \cup (P_{\varepsilon_i, x_j} \cap P'_{\varepsilon_i, x_j}) = P_{\varepsilon_i, x_j}$.

Using these observations and 1(iii), we have

$$\mathcal{Q}_\xi[P_{\varepsilon_i, x_j}] = \mathcal{Q}_\xi[P_{\varepsilon_i, x_j} \setminus P'_{\varepsilon_i, x_j} \cup (P_{\varepsilon_i, x_j} \cap P'_{\varepsilon_i, x_j})] = \mathcal{Q}_\xi[P_{\varepsilon_i, x_j} \setminus P'_{\varepsilon_i, x_j}] + \mathcal{Q}_\xi[P_{\varepsilon_i, x_j} \cap P'_{\varepsilon_i, x_j}].$$

The result follows immediately. \square

Proof of Lemma 1(v). First, let $p \in P_{\varepsilon_i, x_j}(b) \cap P_{\varepsilon_i, x_j}(b')$. Then p is in both $P_{\varepsilon_i, x_j}(b)$ and $P_{\varepsilon_i, x_j}(b')$. This can only be if p satisfies both b and b' . But then p is also in $P_{\varepsilon_i, x_j}(b \wedge b')$. Second, let $p \in P_{\varepsilon_i, x_j}(b \wedge b')$. Then p satisfies both b and b' . Thus $p \in P_{\varepsilon_i, x_j}(b)$ and $p \in P_{\varepsilon_i, x_j}(b')$. But then $p \in P_{\varepsilon_i, x_j}(b) \cap P_{\varepsilon_i, x_j}(b')$. The result now follows from the above two observations. \square

Proof of Lemma 1(vi). First, let $p \in P_{\varepsilon_i, x_j}(b \vee b')$. Then p satisfies either b , or b' or both.

- If p satisfies b , then $p \in P_{\varepsilon_i, x_j}(b)$ and thus $p \in P_{\varepsilon_i, x_j}(b) \cup (P_{\varepsilon_i, x_j}(b') \setminus P_{\varepsilon_i, x_j}(b \wedge b'))$.
- If p satisfies b and b' , then p satisfies b and thus $p \in P_{\varepsilon_i, x_j}(b)$ and therefore $p \in P_{\varepsilon_i, x_j}(b) \cup (P_{\varepsilon_i, x_j}(b') \setminus P_{\varepsilon_i, x_j}(b \wedge b'))$.
- If p satisfies b' but not b , then $p \in P_{\varepsilon_i, x_j}(b') \setminus P_{\varepsilon_i, x_j}(b \wedge b')$ and thus $p \in P_{\varepsilon_i, x_j}(b) \cup (P_{\varepsilon_i, x_j}(b') \setminus P_{\varepsilon_i, x_j}(b \wedge b'))$.

Therefore, $p \in P_{\varepsilon_i, x_j}(b \vee b') \Rightarrow p \in P_{\varepsilon_i, x_j}(b) \cup (P_{\varepsilon_i, x_j}(b') \setminus P_{\varepsilon_i, x_j}(b \wedge b'))$.

Second, let $p \in P_{\varepsilon_i, x_j}(b) \cup (P_{\varepsilon_i, x_j}(b') \setminus P_{\varepsilon_i, x_j}(b \wedge b'))$.

- If $p \in P_{\varepsilon_i, x_j}(b)$, then p satisfies b or p satisfies b and b' .
- If $p \in P_{\varepsilon_i, x_j}(b') \setminus P_{\varepsilon_i, x_j}(b \wedge b')$, then p satisfies b' but not b .
- $P_{\varepsilon_i, x_j}(b)$ and $P_{\varepsilon_i, x_j}(b') \setminus P_{\varepsilon_i, x_j}(b \wedge b')$ are disjoint and thus p never falls into both.

Thus, p always satisfies b or b' or both, and thus $p \in P_{\varepsilon_i, x_j}(b) \cup (P_{\varepsilon_i, x_j}(b') \setminus P_{\varepsilon_i, x_j}(b \wedge b')) \Rightarrow p \in P_{\varepsilon_i, x_j}(b \vee b')$. Both points together prove the statement. \square

Proof of Lemma 1(vii). First, let $p \in P_{\varepsilon_i, x_j}(b \wedge \neg b')$. Then p satisfies b but not b' . Thus $p \in P_{\varepsilon_i, x_j}(b)$ but $p \notin P_{\varepsilon_i, x_j}(b \wedge b')$. Therefore, $p \in P_{\varepsilon_i, x_j}(b) \setminus P_{\varepsilon_i, x_j}(b \wedge b')$. Second, let $p \in P_{\varepsilon_i, x_j}(b) \setminus P_{\varepsilon_i, x_j}(b \wedge b')$. Then p satisfies $b \wedge \neg(b \wedge b')$. A truth table then shows that p satisfies $b \wedge \neg b'$ and therefore $p \in P_{\varepsilon_i, x_j}(b \wedge \neg b')$. Both points together prove the statement. \square

Proof of Lemma 1(viii). Note that $P_{\varepsilon_i, x_j}(\neg x_k) = \mathcal{P}_{\varepsilon_i, x_j} \setminus P_{\varepsilon_i, x_j}(x_k)$. Then by Property 1(iv) we have

$$\begin{aligned} \mathcal{Q}_\xi[P_{\varepsilon_i, x_j}(\neg x_k)] &= \mathcal{Q}_\xi[\mathcal{P}_{\varepsilon_i, x_j} \setminus P_{\varepsilon_i, x_j}(x_k)] = \mathcal{Q}_\xi[\mathcal{P}_{\varepsilon_i, x_j}] - \mathcal{Q}_\xi[P_{\varepsilon_i, x_j} \cap P_{\varepsilon_i, x_j}(x_k)] \\ &= \mathcal{Q}_\xi[\mathcal{P}_{\varepsilon_i, x_j}] - \mathcal{Q}_\xi[P_{\varepsilon_i, x_j}(x_k)]. \end{aligned} \quad \square$$

B.2 Proofs of Main Results

Proof of Theorem 1. Under the conditions of Theorem 1, we can define the causal effect of ε_i on x_j as

$$\mathcal{C}_{\varepsilon_i, x_j}(\boldsymbol{\epsilon}^{(j)}) = \mathbb{E}[x_j^*(\boldsymbol{\epsilon}^{(j)}) - x_j^*(\mathbf{0})],$$

which can then be written as

$$\begin{aligned} \mathcal{C}_{\varepsilon_i, x_j}(\boldsymbol{\epsilon}^{(j)}) &= \sum_{k_1=1}^{j-1} \left\{ \mathbf{B}_{j, k_1} \mathbb{E}[x_{k_1}^*(\boldsymbol{\epsilon}^{(j \cdot k_1)}) - x_{k_1}^*(\mathbf{0}_{\eta(k_1)})] \right\} + \boldsymbol{\Omega}_{j, i} \boldsymbol{\epsilon}_{\eta(j)}^{(j)} \\ &= \sum_{k_1=1}^{j-1} \left\{ \mathbf{B}_{j, k_1} \mathcal{C}_{\varepsilon_i, x_{k_1}}(\boldsymbol{\epsilon}^{(j \cdot k_1)}) \right\} + \boldsymbol{\Omega}_{j, i} \boldsymbol{\epsilon}_{\eta(j)}^{(j)} \\ &= \boldsymbol{\Omega}_{j, i} \boldsymbol{\epsilon}_{\eta(j)}^{(j)} + \sum_{k_1=1}^{j-1} \mathbf{B}_{j, k_1} \boldsymbol{\Omega}_{k_1, i} \boldsymbol{\epsilon}_{\eta(k_1)}^{(j \cdot k_1)} + \sum_{k_1=1}^{j-1} \sum_{k_2=1}^{k_1-1} \left\{ \mathbf{B}_{j, k_1} \mathbf{B}_{k_1, k_2} \mathcal{C}_{\varepsilon_i, x_{k_2}}(\boldsymbol{\epsilon}^{(j \cdot k_1 \cdot k_2)}) \right\}. \end{aligned}$$

Denote for $l = 0, \dots, j-1$,

$$S(l) = \begin{cases} \boldsymbol{\Omega}_{j, i} \boldsymbol{\epsilon}_{\eta(j)}^{(j)} & l = 0 \\ \sum_{k_1=1}^{j-1} \sum_{k_2=1}^{k_1-1} \dots \sum_{k_l=1}^{k_{l-1}-1} \mathbf{B}_{j, k_1} \mathbf{B}_{k_1, k_2} \dots \mathbf{B}_{k_{l-1}, k_l} \boldsymbol{\Omega}_{k_l, i} \boldsymbol{\epsilon}_{\eta(k_l)}^{(j \cdot k_1 \cdot \dots \cdot k_{l-1} \cdot k_l)} & l \geq 1. \end{cases}$$

It then follows that

$$\mathcal{C}_{\varepsilon_i, x_j}(\boldsymbol{\epsilon}^{(j)}) = \sum_{l=1}^{j-1} S(l). \quad (\text{B.1})$$

The following observations now lead to the equivalence proof:

1. $S(l)$ enumerates all paths that include l intermediate variables.
2. Due to the structure of \mathbf{B} , there never exists an edge from node $x_r \rightarrow x_s$ if $r > s$. Thus, there exists no path from ε_i to x_j that has more than $j-1$ intermediate variables.
3. This last observation implies that the right-hand-side of equation (B.1) enumerates all paths that exist in $\mathcal{G}(\mathbf{B}, \boldsymbol{\Omega})$ from ε_i to x_j .
4. The product $\mathbf{B}_{j, k_1} \mathbf{B}_{k_1, k_2} \dots \mathbf{B}_{k_{l-1}, k_l} \boldsymbol{\Omega}_{k_l, i}$ in $S(l)$ is the product of path coefficients along the path $\varepsilon_i \rightarrow x_{k_l} \rightarrow \dots \rightarrow x_{k_1} \rightarrow x_j$ and thus equals the path-specific effect of this path.
5. $\boldsymbol{\epsilon}_{\eta(k_l)}^{(j \cdot k_1 \cdot \dots \cdot k_{l-1} \cdot k_l)}$ acts as a path selector. If $\boldsymbol{\epsilon}_{\eta(k_l)}^{(j \cdot k_1 \cdot \dots \cdot k_{l-1} \cdot k_l)} = 0$, such that the path is not selected, then the term $\mathbf{B}_{j, k_1} \mathbf{B}_{k_1, k_2} \dots \mathbf{B}_{k_{l-1}, k_l} \boldsymbol{\Omega}_{k_l, i}$ drops out of the

right-hand-side of equation (B.1).

According to observations 1 to 3, the potential outcomes assignment vector has as many entries as there exist paths in the graph $\mathcal{G}(\mathbf{B}, \boldsymbol{\Omega})$. Next, take a set of paths P_{ε_i, x_j} as given. By observations 4 and 5, we can set the elements in the potential outcomes assignment vector $\boldsymbol{\epsilon}^{(j)}$ selecting the paths in P_{ε_i, x_j} equal to ξ and all other elements to zero. This then implies $\mathcal{Q}_\xi(P_{\varepsilon_i, x_j}) = \mathcal{C}_{\varepsilon_i, x_j}(\boldsymbol{\epsilon}^{(j)})$. Finally, take a potential outcomes assignment vector $\boldsymbol{\epsilon}^{(j)}$ with $\epsilon_k^{(j)} \in \{\xi, 0\}$ as given. Then, by observations 3 and 5, this potential outcomes assignment vector selects a set of paths P_{ε_i, x_j} such that $\mathcal{C}_{\varepsilon_i, x_j}(\boldsymbol{\epsilon}^{(j)}) = \mathcal{Q}_\xi(P_{\varepsilon_i, x_j})$. \square

Proof of Theorem 2(i). Recall from Theorem 1 that $\mathcal{C}_{\varepsilon_i, x_j}(\boldsymbol{\epsilon}^{(j)}) = \mathcal{Q}_\xi[P_{\varepsilon_i, x_j}]$. Taking $\boldsymbol{\epsilon}^{(j)} = \xi \mathbf{1}_{\eta(j)}$ immediately results in $P_{\varepsilon_i, x_j} = \mathcal{P}_{\varepsilon_i, x_j}$. This, in turn, implies by Theorem 1 that $\mathcal{C}_{\varepsilon_i, x_j}(\xi \mathbf{1}_{\eta(j)}) = \mathcal{Q}_\xi(\mathcal{P}_{\varepsilon_i, x_j})$. Next, note that $\mathcal{C}_{\varepsilon_i, x_j}(\xi \mathbf{1}_{\eta(j)}) = \mathbb{E}[x_j | \varepsilon_i = \xi] - \mathbb{E}[x_j | \varepsilon_i = 0] = \xi \Phi_{j,i}$, which completes the proof. \square

Proof of Theorem 2(ii). As $P_{\varepsilon_i, x_j}^{(1)}, \dots, P_{\varepsilon_i, x_j}^{(k)}$ is a partition, $P_{\varepsilon_i, x_j}^{(1)}, \cup_{r=2}^k P_{\varepsilon_i, x_j}^{(r)}$ is a partition as well. By the first part we therefore have

$$\xi \Phi_{j,i} = \mathcal{Q}_\xi(\mathcal{P}_{\varepsilon_i, x_j}) = \mathcal{Q}_\xi[P_{\varepsilon_i, x_j}^{(1)} \cup (\cup_{r=2}^k P_{\varepsilon_i, x_j}^{(r)})].$$

Since $P_{\varepsilon_i, x_j}^{(1)}$ and $\cup_{r=2}^k P_{\varepsilon_i, x_j}^{(r)}$ are disjoint, Lemma 1(iii) implies

$$\mathcal{Q}_\xi[P_{\varepsilon_i, x_j}^{(1)} \cup (\cup_{r=2}^k P_{\varepsilon_i, x_j}^{(r)})] = \mathcal{Q}_\xi[P_{\varepsilon_i, x_j}^{(1)}] + \mathcal{Q}_\xi[\cup_{r=2}^k P_{\varepsilon_i, x_j}^{(r)}].$$

Applying the same logic recursively to $\mathcal{Q}_\xi[\cup_{r=2}^k P_{\varepsilon_i, x_j}^{(r)}]$ results in

$$\xi \Phi_{j,i} = \sum_{r=1}^k \mathcal{Q}_\xi(P_{\varepsilon_i, x_j}^{(r)}),$$

completing the proof of the second part. \square

Proof of Theorem 2(iii). Note that each element in the potential outcomes assignment vector $\boldsymbol{\epsilon}^{(j)}$ selects whether a specific path is active or not. Thus, for each collection $P_{\varepsilon_i, x_j}^{(r)}$ there exists a potential outcomes assignment vector \mathbf{e}_r that has a ξ at those elements selecting that paths present in $P_{\varepsilon_i, x_j}^{(r)}$ and 0 at all other elements. Since no path can be present in two collections of the partition, $\sum_{r=1}^k \mathbf{e}_r = \xi \mathbf{1}_{\eta(j)}$. Applying Theorems 1 and 2(ii) yields $\sum_{r=1}^k \mathcal{C}_{\varepsilon_i, x_j}(\mathbf{e}_m) = \xi \Phi_{j,i}$. \square

Proof of Theorem 3(i). After substituting $\mathbf{Q}'\mathbf{A}_i^* = \bar{\mathbf{A}}$, $\mathbf{Q}'\boldsymbol{\Psi}_i\mathbf{Q} = \bar{\boldsymbol{\Psi}}_i$ and $\gamma_t = \mathbf{Q}'\boldsymbol{\varepsilon}_t$, equation (8) can be written as

$$\mathbf{L}\mathbf{y}_t^* = \sum_{i=1}^{\ell} \bar{\mathbf{A}}_i \mathbf{y}_{t-i}^* + \gamma_t + \sum_{j=1}^q \bar{\boldsymbol{\Psi}}_j \gamma_t. \quad (\text{B.2})$$

Since \mathbf{L} is lower-triangular, this system can be obtained from the reduced form system using a Cholesky identification scheme following the ordering in the transmission matrix \mathbf{T} .

Following similar steps to Appendix A, the system (B.2) can be written as

$$\mathbf{x} = \tilde{\mathbf{B}}\mathbf{x} + \tilde{\boldsymbol{\Omega}}\boldsymbol{\gamma}, \quad (\text{B.3})$$

where $\boldsymbol{\gamma} = (\gamma'_t, \dots, \gamma'_{t+h})'$, $\mathbf{x} = (\mathbf{y}'_t, \dots, \mathbf{y}'_{t+h})'$ and $\tilde{\mathbf{B}} = \mathbf{B}$, and

$$\tilde{\boldsymbol{\Omega}} = \begin{bmatrix} \mathbf{D} & 0 & \dots & 0 \\ \mathbf{D}\bar{\boldsymbol{\Psi}}_1 & \mathbf{D} & \dots & 0 \\ \vdots & \ddots & \ddots & \vdots \\ \mathbf{D}\bar{\boldsymbol{\Psi}}_h & \dots & \mathbf{D}\bar{\boldsymbol{\Psi}}_1 & \mathbf{D} \end{bmatrix}, \quad (\text{B.4})$$

with $\bar{\mathbf{A}}_i = \mathbf{O}$ for $i > \ell$, and $\bar{\boldsymbol{\Psi}}_j = \mathbf{O}$ for $j > q$, and $\mathbf{D} = \text{diag}(\mathbf{L})^{-1}$, where $\text{diag}(\mathbf{X})$ is a diagonal matrix of the diagonal of \mathbf{X} .

Since $\mathbf{B} = \tilde{\mathbf{B}}$, the system (B.3) induces a graph $\mathcal{G}(\tilde{\mathbf{B}}, \tilde{\boldsymbol{\Omega}})$ that has the same path-coefficients for any edge $x_j \rightarrow x_i$ as the graph $\mathcal{G}(\mathbf{B}, \boldsymbol{\Omega})$.

Because the shocks in $\boldsymbol{\gamma}$ are uncorrelated, we can use the graph $\mathcal{G}(\tilde{\mathbf{B}}, \tilde{\boldsymbol{\Omega}})$ to investigate the effect of the shock γ_i on x_j along all paths in the graph, $\mathcal{P}_{\gamma_i, x_j}$. This effect is given by the total path-specific effect

$$\sum_{p \in \mathcal{P}_{\gamma_i, x_j}} \prod_{u \rightarrow v \in p} \tilde{\omega}_{u,v}, \quad (\text{B.5})$$

where $\tilde{\omega}_{u,v}$ is the path coefficient of the edge connecting u to v .

Since $\tilde{\boldsymbol{\Omega}}$ is diagonal, any path in $\mathcal{P}_{\gamma_i, x_j}$ must always first go into x_i before it can go through any other variables. Thus equation (B.5) can also be written as

$$\tilde{\omega}_{\gamma_i, x_i} \sum_{p \in \mathcal{P}_{x_i, x_j}} \prod_{u \rightarrow v \in p} \tilde{\omega}_{u,v}. \quad (\text{B.6})$$

Because, $\tilde{\mathbf{B}} = \mathbf{B}$, all path coefficients along paths connecting x_k to x_l for all k, l , are the same as in the graph $\mathcal{G}(\mathbf{B}, \boldsymbol{\Omega})$, $\tilde{\omega}_{u,v} = \omega_{u,v}$ for all $u \neq \gamma_i$. Thus, (B.6)

can also be written as

$$\tilde{\omega}_{\gamma_i, x_i} = \sum_{p \in \mathcal{P}_{x_i, x_j}} \prod_{u \rightarrow v \in p} \omega_{u, v}. \quad (\text{B.7})$$

Letting γ_i take the role of ε_i in Theorem 2, one can show that the total path-specific effect of $\mathcal{P}_{\gamma_i, x_j}$ in the graph $\mathcal{G}(\tilde{\mathbf{B}}, \tilde{\mathbf{\Omega}})$ equals the total effect of γ_i on x_j , which is given by the impulse response matrix

$$\tilde{\Phi}_{j, i} = [(\mathbf{I} - \tilde{\mathbf{B}})^{-1} \tilde{\mathbf{\Omega}}]_{j, i} = [(\mathbf{I} - \mathbf{B})^{-1} \tilde{\mathbf{\Omega}}]_{j, i}. \quad (\text{B.8})$$

Similarly, the effect of γ_i on x_i , which consists of only the direct edge $\gamma_i \rightarrow x_i$ and thus equals $\tilde{\omega}_{\gamma_i, x_i}$, is a total effect, and equal to the impulse response of γ_i on x_i ,

$$\tilde{\Phi}_{i, i} = [(\mathbf{I} - \mathbf{B})^{-1} \tilde{\mathbf{\Omega}}]_{i, i}. \quad (\text{B.9})$$

By combining (B.7), (B.8) and (B.9),

$$\tilde{\Phi}_{i, i} \sum_{p \in \mathcal{P}_{x_i, x_j}} \prod_{u \rightarrow v \in p} \omega_{u, v} = \tilde{\Phi}_{j, i}. \quad (\text{B.10})$$

Rearranging, (B.10) gives the final result,

$$\mathcal{Q}_1(P_{x_i, x_j}) = \sum_{p \in \mathcal{P}_{x_i, x_j}} \prod_{u \rightarrow v \in p} \omega_{u, v} = \tilde{\Phi}_{j, i} \tilde{\Phi}_{i, i}^{-1}. \quad (\text{B.11})$$

To complete the proof, observe that since (B.2) is the system obtained from a Cholesky identification scheme following the ordering given in \mathbf{T} , the impulse response matrix $\tilde{\Phi} = (\mathbf{I} - \mathbf{B})^{-1} \tilde{\mathbf{\Omega}}$ is given by a Cholesky identification following the ordering given in \mathbf{T} . \square

Proof of Theorem 3(ii). Let b be a Boolean formula. We say b is in disjunctive normal form (DNF) if b can be written as

$$b = b_1 \vee b_2 \vee \dots \vee b_n,$$

where b_i includes only conjunctions, \wedge , and negations, \neg . Further, we say b can be written in DNF_n if b can be written in disjunctive normal form involving only $n - 1$ disjunctions, \vee .

According to Theorem 3.8.8 in Chiswell and Hodges (2007) and Theorem 2.1 in Rautenberg (2010), every Boolean formula b can be written in DNF. Thus, for every Boolean formula there exists a $k \in \mathbb{N}$ such that b can be written in DNF_k . Additionally, for any collection of paths $P_{\varepsilon_i, x_j} \subseteq \mathcal{P}_{\varepsilon_i, x_j}$ there exists a

boolean formula b such that $P_{\varepsilon_i, x_j}(b) = P_{\varepsilon_i, x_j}$. Thus, to prove part two of Theorem 3 it suffices to show that for any DNF_k with $k \in \mathbb{N}$, there exists a function $f : \mathbb{R}^{hK \times hK} \times \mathbb{R}^{hk \times hk} \rightarrow \mathbb{R}$ such that $\mathcal{Q}_\xi(P_{\varepsilon_i, x_j}(b)) = f(\Phi, \tilde{\Phi})$. We will prove this by induction.

Let $k = 1$ such that the Boolean formula b consists of only conjunctions and negations; the Boolean formula b is DNF_1 . If b has no negations, then Lemma 1(ii) with Theorems 2 and 3(i) imply that there exists a function f such that $\mathcal{Q}_\xi(P_{\varepsilon_i, x_j}(b)) = f(\Phi, \tilde{\Phi})$. If b has a single negation then we may write $b = \tilde{b} \wedge \neg x_r$ for some variable x_r . Then

$$\begin{aligned} \mathcal{Q}_\xi[P_{\varepsilon_i, x_j}(b)] &= \mathcal{Q}_\xi[P_{\varepsilon_i, x_j}(\tilde{b} \wedge \neg x_r)] = \mathcal{Q}_\xi[P_{\varepsilon_i, x_j}(\tilde{b}) \setminus P_{\varepsilon_i, x_j}(\tilde{b} \wedge x_r)] \\ &= \mathcal{Q}_\xi[P_{\varepsilon_i, x_j}(\tilde{b})] - \mathcal{Q}_\xi[P_{\varepsilon_i, x_j}(\tilde{b} \wedge x_r)]. \end{aligned}$$

The second line above follows by Lemma 1(vii) while the last line follows by Lemma 1(iv) and 1(v). Since \tilde{b} and $\tilde{b} \wedge x_r$ are Boolean formulas consisting of only conjunctions, there exist functions f_1 and f_2 such that $\mathcal{Q}_\xi(P_{\varepsilon_i, x_j}(\tilde{b})) = f_1(\Phi, \tilde{\Phi})$ and $\mathcal{Q}_\xi(P_{\varepsilon_i, x_j}(\tilde{b} \wedge x_r)) = f_2(\Phi, \tilde{\Phi})$. Thus, let $f(\Phi, \tilde{\Phi}) = f_1(\Phi, \tilde{\Phi}) - f_2(\Phi, \tilde{\Phi})$. Then $\mathcal{Q}_\xi(P_{\varepsilon_i, x_j}(b)) = f(\Phi, \tilde{\Phi})$.

Finally, if b consists of m negations, then we may write $b = \bar{b} \wedge \neg x_r$ for some variable x_r , where \bar{b} consists of $m - 1$ negations. We can thus again write

$$\begin{aligned} \mathcal{Q}_\xi[P_{\varepsilon_i, x_j}(b)] &= \mathcal{Q}_\xi[P_{\varepsilon_i, x_j}(\bar{b} \wedge \neg x_r)] \\ &= \mathcal{Q}_\xi[P_{\varepsilon_i, x_j}(\bar{b}) \setminus P_{\varepsilon_i, x_j}(\bar{b} \wedge x_r)] \\ &= \mathcal{Q}_\xi[P_{\varepsilon_i, x_j}(\bar{b})] - \mathcal{Q}_\xi[P_{\varepsilon_i, x_j}(\bar{b} \wedge x_r)]. \end{aligned}$$

By the induction hypothesis, there exists a function f_1 such that $\mathcal{Q}_\xi(P_{\varepsilon_i, x_j}(\bar{b})) = f_1(\Phi, \tilde{\Phi})$. Additionally, since $\bar{b} \wedge x_r$ consists of only $m - 1$ negations, the induction hypothesis also implies that there exists a function f_2 such that $\mathcal{Q}_\xi(P_{\varepsilon_i, x_j}(\bar{b} \wedge x_r)) = f_2(\Phi, \tilde{\Phi})$. Thus, let $f(\Phi, \tilde{\Phi}) = f_1(\Phi, \tilde{\Phi}) - f_2(\Phi, \tilde{\Phi})$. Then $\mathcal{Q}_\xi(P_{\varepsilon_i, x_j}(b)) = f(\Phi, \tilde{\Phi})$. Thus, if b is DNF_1 with $m \in \mathbb{N}$ negations, then there exists a function f such that $\mathcal{Q}_\xi(P_{\varepsilon_i, x_j}(b)) = f(\Phi, \tilde{\Phi})$.

Next, suppose there exists a function f such that $\mathcal{Q}_\xi(P_{\varepsilon_i, x_j}(\bar{b})) = f(\Phi, \tilde{\Phi})$ if \bar{b} is DNF_k and let the Boolean formula b be DNF_{k+1} . We can then write $b = b_1 \vee \bar{b}$ where b_1 is DNF_1 . By Lemma 1(vi), it follows that

$$P_{\varepsilon_i, x_j}(b) = P_{\varepsilon_i, x_j}(b_1) \cup (P_{\varepsilon_i, x_j}(\bar{b}) \setminus P_{\varepsilon_i, x_j}(b_1 \wedge \bar{b})).$$

Note that $P_{\varepsilon_i, x_j}(b_1)$ and $P_{\varepsilon_i, x_j}(\bar{b}) \setminus P_{\varepsilon_i, x_j}(b_1 \wedge \bar{b})$ are disjoint. Thus, by Lemma 1(iii)

and 1(iv),

$$\mathcal{Q}_\xi(P_{\varepsilon_i, x_j}(b)) = \underbrace{\mathcal{Q}_\xi(P_{\varepsilon_i, x_j}(b_1))}_{\text{DNF}_1} + \underbrace{\mathcal{Q}_\xi(P_{\varepsilon_i, x_j}(\bar{b}))}_{\text{DNF}_k} - \underbrace{\mathcal{Q}_\xi(P_{\varepsilon_i, x_j}(b_1 \wedge \bar{b}))}_{\text{DNF}_k}.$$

Since there exists a function f_1 such that $\mathcal{Q}_\xi(P_{\varepsilon_i, x_j}(b_1)) = f_1(\Phi, \tilde{\Phi})$, and since the induction hypothesis implies that there exist functions f_2 and f_3 such that $\mathcal{Q}_\xi(P_{\varepsilon_i, x_j}(\bar{b})) = f_2(\Phi, \tilde{\Phi})$ and $\mathcal{Q}_\xi(P_{\varepsilon_i, x_j}(b_1 \wedge \bar{b})) = f_3(\Phi, \tilde{\Phi})$, there exists a function $f(\Phi, \tilde{\Phi}) = f_1(\Phi, \tilde{\Phi}) + f_2(\Phi, \tilde{\Phi}) - f_3(\Phi, \tilde{\Phi})$ such that $\mathcal{Q}_\xi(P_{\varepsilon_i, x_j}(b)) = f(\Phi, \tilde{\Phi})$.

We can then conclude that, for any $n \in \mathbb{N}$ and any Boolean formula b being DNF_n , there exists a function f such that $\mathcal{Q}_\xi(P_{\varepsilon_i, x_j}(b)) = f(\Phi, \tilde{\Phi})$. This concludes the proof. \square

Proof of Theorem 4. Theorem 3 shows that there always exists a function $f : \mathbb{R}^{hK \times hK} \times \mathbb{R}^{hK \times hK} \rightarrow \mathbb{R}$ such that $\mathcal{Q}_\xi(P_{\varepsilon_i, x_j}) = f(\Phi, \tilde{\Phi})$. This function is found by recursively applying Lemma 1(i) through 1(viii). The only time this recursion stops is at Lemma 1(i), 1(ii) or 1(viii). It thus suffices to show that Lemmas 1(i), 1(ii) and 1(viii) only require $\Phi_{\cdot, i}$ and $\tilde{\Phi}$ for the calculation of the transmission effect.

For Lemma 1(i) note that by Theorem 3(i) $\mathcal{Q}_\xi(\mathcal{P}_{x_k, x_j}) = \tilde{\Phi}_{j, k}$ and by Theorem 2 $\mathcal{Q}_\xi(\mathcal{P}_{\varepsilon_i, x_k}) = \Phi_{k, i}$. Thus, Lemma 1(i) only requires $\Phi_{\cdot, i}$ and $\tilde{\Phi}$ for the calculation of transmission effects.

For Lemma 1(ii) note that by Theorem 3(i) $\mathcal{Q}_\xi(\mathcal{P}_{x_{i_r}, x_{i_s}}) = \tilde{\Phi}_{i_s, i_r}$ for $s > r$ and $0 < s, r \leq k$. Additionally, by the same Theorem $\mathcal{Q}_\xi(\mathcal{P}_{x_{i_k}, x_j}) = \tilde{\Phi}_{j, i_k}$. Lastly, by Theorem 2, $\mathcal{Q}_\xi(\mathcal{P}_{\varepsilon_i, x_{i_1}}) = \Phi_{i_1, i}$. Thus, Lemma 1(ii) only requires $\Phi_{\cdot, 1}$ and $\tilde{\Phi}$ for the calculation of transmission effects.

Finally, for Lemma 1(viii) note that $\mathcal{Q}_\xi(P_{\varepsilon_i, x_j}(x_k)) = \mathcal{Q}_\xi(\mathcal{P}_{\varepsilon_i, x_k})\mathcal{Q}_1(\mathcal{P}_{x_k, x_j})$ by Lemma 1(i), which only requires $\Phi_{\cdot, i}$ and $\tilde{\Phi}$ for the calculation of transmission effects. Additionally, by Theorem 2, $\mathcal{Q}_\xi(\mathcal{P}_{\varepsilon_i, x_j}) = \Phi_{j, i}$.

Thus, Lemma 1(i), 1(ii) and 1(viii) only require $\Phi_{\cdot, i}$ and $\tilde{\Phi}$ for the calculation of transmission effects. Therefore, the calculation of any transmission effect requires only the i th column of Φ , $\Phi_{\cdot, i}$, to be structurally identified. \square

Appendix C Computing Transmission Effects

In this section we discuss how transmission effects can be computed in practice. Section C.1 discusses computational issues and proposes an efficient algorithm computing transmission effects. Section C.2 establishes the correctness of the

proposed approach. Section C.3 discusses how uncertainty around point estimates can be quantified using a Frequentist or Bayesian approach.

C.1 Efficient Computational Approaches

Section 3 shows that given a collection of paths P_{ε_i, x_j} constituting a transmission channel, transmission effects can be calculated as the total path-specific effect of P_{ε_i, x_j} , $\mathcal{Q}_\xi(P_{\varepsilon_i, x_j})$. This is an efficient method if the collection of paths is known. However, often times it is more intuitive to define transmission channels in terms of which variable may or may not lie on a path, i.e. it is more natural to define transmission channels in terms of Boolean statements (see Appendix B.1). Given such a definition, the collection of paths must first be found before the total path-specific effect can be calculated. Finding all paths corresponding to a Boolean statement is computationally costly, especially for models with many variables or for effects over many horizons - in either case the number of paths grows exponentially. Thus, first finding all paths and then calculating the total path-specific effect is inefficient in those cases.

An alternative approach is to directly use impulse response functions; Theorem 3 states that all transmission effects can be computed using a combination of IRFs. Given a transmission channel P_{ε_i, x_j} implicitly defined using a Boolean formula b , this can be made operational, by first using Lemma 1 to split the transmission effect of P_{ε_i, x_j} into terms involving the total path-specific effects of simpler collections of paths - those that use all paths connecting two variables or a shock and a variable. Each term can then be calculated using Theorem 2 and 3 as an impulse response.

The above approach has the advantage that it allows for alternative methods to compute IRFs such as local projections (Jordà, 2005), but it requires a full simplification of the Boolean statement, i.e. the transmission effect must be simplified to terms involving collections of all paths connecting two variables or a variable and a shock. This is computationally expensive and a more efficient algorithm could be obtained if full simplification was not required - if NOTs (\neg) would not have to be simplified. This can be achieved by combining Lemma 1 with insights obtained from the graphical representation $\mathcal{G}(\mathbf{B}, \mathbf{\Omega})$.

Suppose the Boolean formula is $b = x_k$ ($k < j$). Then all paths of the transmission channel P_{ε_i, x_j} implied by the Boolean statement b must go through x_k . Thus, if we were to remove all paths p in the graph $\mathcal{G}(\mathbf{B}, \mathbf{\Omega})$ that did not go through x_k , then the resulting graph $\mathcal{G}(\bar{\mathbf{B}}, \bar{\mathbf{\Omega}})$ would only contain paths going through x_k .

The total effect of the structural shock ε_i on x_j in the graph $\mathcal{G}(\bar{\mathbf{B}}, \bar{\mathbf{\Omega}})$ would then use all paths connecting ε_i and x_j and going through x_k but no paths that do not go through x_k . By Theorem 2 this total effect is given by $\bar{\Phi}_{j,i} = (\mathbf{I} - \bar{\mathbf{B}})_{j,\cdot}^{-1} \bar{\mathbf{\Omega}}_{\cdot,i}$. Because moving from $\mathcal{G}(\mathbf{B}, \mathbf{\Omega})$ to $\mathcal{G}(\bar{\mathbf{B}}, \bar{\mathbf{\Omega}})$ only removes edges and does not change path coefficients, the total effect $\bar{\Phi}_{j,i}$ equals the transmission effect of the transmission channel P_{ε_i, x_j} . A similar logic can be applied to Boolean formulas $b = \neg x_k$ ($k < j$) implying that paths cannot go through x_k ; this time, all paths that go through x_k are removed. We can generalise this logic to any Boolean formula of the form $b = \bigwedge_{k \in N_1} x_k \bigwedge_{k \in N_2} \neg x_k$ with $k < j \forall k \in N_1 \cup N_2$, resulting in Algorithm 1.

Algorithm 1: Calculating the transmission effect of $b = \bigwedge_{k \in N_1} x_k \bigwedge_{k \in N_2} \neg x_k$ from shock ε_i to x_j

Input: Boolean statement $b = \bigwedge_{k \in N_1} x_k \bigwedge_{k \in N_2} \neg x_k$ with

$k < j \forall k \in N_1 \cup N_2$, matrices \mathbf{B} and $\mathbf{\Omega}_{\cdot,i}$, shock size ξ

Output: Transmission effect $\mathcal{Q}_\xi(P_{\varepsilon_i, x_j})$ where P_{ε_i, x_j} is implicitly defined by b

$\bar{\mathbf{B}} \leftarrow \mathbf{B}$

$\bar{\mathbf{\Omega}}_{\cdot,i} \leftarrow \mathbf{\Omega}_{\cdot,i}$

for $k \in N_1$ **do**

$\bar{\mathbf{B}}_{r,s} \leftarrow 0$ if $r > k$ and $s < k$
 $\bar{\mathbf{\Omega}}_{r,i} \leftarrow 0$ if $r > k$

end

for $k \in N_2$ **do**

$\bar{\mathbf{B}}_{k,s} \leftarrow 0$ if $s < k$
 $\bar{\mathbf{\Omega}}_{k,i} \leftarrow 0$

end

return $\xi(\mathbf{I} - \bar{\mathbf{B}})_{j,\cdot}^{-1} \bar{\mathbf{\Omega}}_{\cdot,i}$

Algorithm 1 requires Boolean formulas of a specific form; however, not all transmission channels can be defined by such a Boolean formula. Thus, Algorithm 1 must be combined with Lemma 1. Lemma 1 is first applied to a Boolean formula b until each term involves Boolean formulas amendable to Algorithm 1. Algorithm 1 can then be used to compute each term. Since Boolean formulas need not be fully simplified - terms can consist of collections of paths that do not contain all paths connecting two variables or a variable and a shock - the combination of Lemma 1 and Algorithm 1 is often more efficient than using IRFs. Additionally, Lemma 2 shows that this method can be applied even if the full graph is not known - only the structural shock whose effects the researcher wants to decompose is known. Thus, unless local projections are being used, the combination of Lemma 1 and

Algorithm 1 has no clear shortcomings compared to using Lemma 1 with IRFs; it is, therefore, oftentimes the preferred approach.

Lemma 2. Let \mathbf{L} be the contemporaneous matrix obtained when using a Cholesky identification scheme following the ordering in \mathbf{T} , $\bar{\mathbf{A}}_i$ be the AR coefficient matrices and $\bar{\Psi}_j$ be the MA coefficient matrices obtained using the same scheme, and suppose $(\mathbf{A}_0^*)_{\cdot,i}^{-1} = \Phi_{1:K,i}$ is identified. Then $\mathbf{Q}'_{\cdot,i} = \mathbf{L}(\mathbf{A}_0^*)_{\cdot,i}^{-1}$, $(\mathbf{Q}'\Psi_j)_{\cdot,i} = \bar{\Psi}_j\mathbf{Q}'_{\cdot,i}$ for all $j = 1, \dots, q$, and

$$\mathbf{B} = \begin{bmatrix} \mathbf{I} - \mathbf{DL} & \mathbf{O} & \dots & \mathbf{O} \\ \mathbf{D}\bar{\mathbf{A}}_1 & \mathbf{I} - \mathbf{DL} & \dots & \mathbf{O} \\ \vdots & \ddots & \ddots & \vdots \\ \mathbf{D}\bar{\mathbf{A}}_h & \dots & \mathbf{D}\bar{\mathbf{A}}_1 & \mathbf{I} - \mathbf{DL} \end{bmatrix} \quad \text{and} \quad \Phi_{\cdot,i} = \begin{bmatrix} \mathbf{D}\mathbf{Q}'_{\cdot,i} \\ \mathbf{D}(\mathbf{Q}'\Psi_1)_{\cdot,i} \\ \vdots \\ \mathbf{D}(\mathbf{Q}'\Psi_h)_{\cdot,h} \end{bmatrix}, \quad (\text{C.1})$$

with $\mathbf{D} = \text{diag}(\mathbf{L})^{-1}$, $\bar{\mathbf{A}}_i = \mathbf{O}$ for $i > \ell$, and $\bar{\Psi}_j = \mathbf{O}$ for all $j > q$.

Proof of Lemma 2. After substituting $\bar{\mathbf{A}}_i = \mathbf{Q}'\mathbf{A}_i^*$ ($i \geq 1$), $\bar{\Psi}_j = \mathbf{Q}'\Psi_j\mathbf{Q}$ ($j \geq 1$) and $\gamma_t = \mathbf{Q}'\varepsilon_t$, 8 can be written as

$$\mathbf{L}\mathbf{y}_t^* = \sum_{i=1}^{\ell} \bar{\mathbf{A}}_i \mathbf{y}_{t-i}^* + \sum_{j=1}^q l \bar{\Psi}_j \gamma_{t-j} + \gamma_t.$$

This is the system obtained using a Cholesky identification scheme following the ordering in \mathbf{T} . We then have $(\mathbf{A}_0^*)_{\cdot,i}^{-1} = (\mathbf{Q}\mathbf{L})_{\cdot,i}^{-1} = \mathbf{L}^{-1}\mathbf{Q}'_{\cdot,i}$ implying $\mathbf{Q}'_{\cdot,i} = \mathbf{L}(\mathbf{A}_0^*)_{\cdot,i}^{-1}$. Similarly, we have $(\mathbf{Q}'\Psi_j)_{\cdot,i} = \mathbf{Q}'\Psi_j\mathbf{Q}\mathbf{Q}'_{\cdot,j} = \bar{\Psi}_j\mathbf{Q}'_{\cdot,i}$. The form of \mathbf{B} and $\Omega_{\cdot,i}$ can then be obtained by substituting the above into equation (10). \square

C.2 Properties of the Computational Algorithm

In this section we prove the correctness of the computational approach suggested in the previous section. More precisely, we will show that combining Lemma 1 with Algorithm 1 correctly computes the transmission effect of any transmission channel. Given that Lemma 1 can be used to split the computation of the transmission effect of a transmission channel P_{ε_i, x_j} implicitly defined by a Boolean statement b into terms involving Boolean formulas (transmission channels) that can be computed using Algorithm 1, it suffices to show that Algorithm 1 correctly computes the transmission effect of a transmission channel indirectly defined by a Boolean formula of the form $b = \bigwedge_{k \in N_1} x_k \bigwedge_{k \in N_2} \neg x_k$ with $k < j \forall k \in N_1 \cup N_2$.

We first prove that the first loop of Algorithm 1 removes all and only paths

p from $\mathcal{G}(\mathbf{B}, \mathbf{\Omega})$ that do not satisfy $\bigwedge_{k \in N_1} x_k$ with $k < j$ for all $k \in N_1$. This is implied by Lemma 3 and 4 below.

Lemma 3. Let $b = x_k$ and $\bar{\mathbf{B}} = \mathbf{B}$, $\bar{\mathbf{\Omega}} = \mathbf{\Omega}$ except that $\bar{\mathbf{B}}_{r,s} = 0$ and $\bar{\mathbf{\Omega}}_{r,i} = 0$ whenever $s < k$ and $r > k$. Then $\mathcal{G}(\bar{\mathbf{B}}, \bar{\mathbf{\Omega}})$ contains all and only paths p in $\mathcal{G}(\mathbf{B}, \mathbf{\Omega})$ that satisfy b .

Proof of Lemma 3. Suppose there was a path p in $\mathcal{G}(\bar{\mathbf{B}}, \bar{\mathbf{\Omega}})$ that did not satisfy b . Then p must have an edge of the kind $x_s \rightarrow x_r$ or $\varepsilon_i \rightarrow x_r$ with $s < k$ and $r > k$. This is a contradiction, because all such edges have been removed. Next, suppose there was a path p in $\mathcal{G}(\mathbf{B}, \mathbf{\Omega})$ not in $\mathcal{G}(\bar{\mathbf{B}}, \bar{\mathbf{\Omega}})$ that does satisfy b . Since moving from $\mathcal{G}(\mathbf{B}, \mathbf{\Omega})$ to $\mathcal{G}(\bar{\mathbf{B}}, \bar{\mathbf{\Omega}})$ only removes edges of the form $x_s \rightarrow x_r$ and $\varepsilon_i \rightarrow x_r$ with $s < k$ and $r > k$, p must have such an edge. This is a contradiction, because it implies that p cannot satisfy b in the first place. \square

Lemma 4. Suppose all paths in $\mathcal{G}(\mathbf{B}, \mathbf{\Omega})$ satisfy the Boolean formula b' and let $b = b' \wedge x_k$. Let $\bar{\mathbf{B}} = \mathbf{B}$ and $\bar{\mathbf{\Omega}} = \mathbf{\Omega}$ except that $\bar{\mathbf{B}}_{r,s} = 0$ and $\bar{\mathbf{\Omega}}_{r,i} = 0$ whenever $s < k$ and $r > k$. Then $\mathcal{G}(\bar{\mathbf{B}}, \bar{\mathbf{\Omega}})$ contains all and only paths in $\mathcal{G}(\mathbf{B}, \mathbf{\Omega})$ that satisfy b .

Proof of Lemma 4. Suppose there was a path p in $\mathcal{G}(\bar{\mathbf{B}}, \bar{\mathbf{\Omega}})$ that did not satisfy b . Then p violates b' or does not go through x_k . By Lemma 3, the latter cannot be the case. Thus, p must violate b' . This is a contradiction, because $\mathcal{G}(\bar{\mathbf{B}}, \bar{\mathbf{\Omega}})$ is obtained from $\mathcal{G}(\mathbf{B}, \mathbf{\Omega})$ by removing paths, and all paths in $\mathcal{G}(\mathbf{B}, \mathbf{\Omega})$ satisfy b' . Next, suppose there was a path p in $\mathcal{G}(\mathbf{B}, \mathbf{\Omega})$ not in $\mathcal{G}(\bar{\mathbf{B}}, \bar{\mathbf{\Omega}})$ that satisfies b . Since all paths in $\mathcal{G}(\mathbf{B}, \mathbf{\Omega})$ already satisfy b' , Lemma 3 implies that this is not possible. \square

Lemma 3 shows that the first iteration of the first loop in Algorithm 1 ends with a graph that contains all and only paths in $\mathcal{G}(\mathbf{B}, \mathbf{\Omega})$ that go through x_{k_1} where we write $N_1 = \{k_1, \dots, k_{N_1}\}$. Lemma 4 then shows that all remaining iterations m end with a graph that contains all and only edges in $\mathcal{G}(\mathbf{B}, \mathbf{\Omega})$ that satisfy $\bigwedge_{i=1}^m x_{k_m}$. Thus, at the end of the first loop, we are left with a graph that contains all and only paths of $\mathcal{G}(\mathbf{B}, \mathbf{\Omega})$ that satisfy $\bigwedge_{k \in N_1} x_k$.

We will next show in Lemmas 5 and 6 that the second loop removes all and only paths from the graph obtained at the end of the first loop that do not satisfy $\bigwedge_{k \in N_2} \neg x_k$.

Lemma 5. Let $b = \neg x_k$ and $\bar{\mathbf{B}} = \mathbf{B}$, $\bar{\mathbf{\Omega}} = \mathbf{\Omega}$ except that $\bar{\mathbf{B}}_{k,s} = 0$ and $\bar{\mathbf{\Omega}}_{k,i} = 0$ whenever $s < k$. Then $\mathcal{G}(\bar{\mathbf{B}}, \bar{\mathbf{\Omega}})$ contains all and only paths p in $\mathcal{G}(\mathbf{B}, \mathbf{\Omega})$ that satisfy b .

Proof of Lemma 5. Suppose there was a path p in $\mathcal{G}(\bar{\mathbf{B}}, \bar{\mathbf{\Omega}})$ that did not satisfy b . Then p must have an edge of the kind $x_s \rightarrow x_k$ or $\varepsilon_i \rightarrow x_k$ with $s < k$. This is a contradiction, because all such edges have been removed. Next, suppose that there was a path p in $\mathcal{G}(\mathbf{B}, \mathbf{\Omega})$ not in $\mathcal{G}(\bar{\mathbf{B}}, \bar{\mathbf{\Omega}})$ that satisfies b . Since moving from $\mathcal{G}(\mathbf{B}, \mathbf{\Omega})$ only removes edges of the kind $x_s \rightarrow x_k$ or $\varepsilon_i \rightarrow x_k$ with $s < k$, p must have such an edge. This is a contradiction, because it would imply that p goes through x_k . \square

Lemma 6. Suppose all paths in $\mathcal{G}(\mathbf{B}, \mathbf{\Omega})$ satisfy the Boolean formula b' and let $b = b' \wedge \neg x_k$. Let $\bar{\mathbf{B}} = \mathbf{B}$ and $\bar{\mathbf{\Omega}} = \mathbf{\Omega}$ except that $\bar{\mathbf{B}}_{k,s} = 0$ and $\bar{\mathbf{\Omega}}_{k,i} = 0$ whenever $s < k$. Then $\mathcal{G}(\bar{\mathbf{B}}, \bar{\mathbf{\Omega}})$ contains all and only paths in $\mathcal{G}(\mathbf{B}, \mathbf{\Omega})$ that satisfy b .

Proof of Lemma 6. Suppose there was a path p in $\mathcal{G}(\bar{\mathbf{B}}, \bar{\mathbf{\Omega}})$ that did not satisfy b . Then p violates b' or does go through x_k . By Lemma 5, the latter cannot be the case. Thus, p must violate b' . This is a contradiction, because $\mathcal{G}(\bar{\mathbf{B}}, \bar{\mathbf{\Omega}})$ is obtained from $\mathcal{G}(\mathbf{B}, \mathbf{\Omega})$ by removing paths, and all paths in $\mathcal{G}(\mathbf{B}, \mathbf{\Omega})$ satisfy b' . Next, suppose there was a path p in $\mathcal{G}(\mathbf{B}, \mathbf{\Omega})$ not in $\mathcal{G}(\bar{\mathbf{B}}, \bar{\mathbf{\Omega}})$ that satisfies b . Since all paths in $\mathcal{G}(\mathbf{B}, \mathbf{\Omega})$ already satisfy b' , Lemma 6 implies that this is not possible. \square

Since the first loop ends with a graph that contains all and only paths in $\mathcal{G}(\mathbf{B}, \mathbf{\Omega})$ that satisfy $\bigwedge_{k \in N_1} x_k$, Lemma 6 shows that the first iteration of the second loop ends with a graph that contains all and only paths in $\mathcal{G}(\mathbf{B}, \mathbf{\Omega})$ that satisfy $\bigwedge_{k \in N_1} x_k \wedge \neg x_{l_1}$ where we write $N_2 = \{l_1, \dots, l_{N_2}\}$. Repeated application of Lemma 6 then shows that at the end of the second loop we are left with a graph that contains all and only paths in $\mathcal{G}(\mathbf{B}, \mathbf{\Omega})$ that satisfy $\bigwedge_{k \in N_1} x_k \wedge_{k \in N_2} \neg x_k$. We are now ready to state the correctness of Algorithm 1.

Lemma 7. Algorithm 1 correctly computes $\mathcal{Q}_\xi(P_{\varepsilon_i, x_j})$ where P_{ε_i, x_j} is implicitly defined by the Boolean formula $b = \bigwedge_{k \in N_1} x_k \wedge_{k \in N_2} \neg x_k$ with $k < j \forall k \in N_1 \cup N_2$.

Proof of Lemma 7. The result follows directly from Lemma 3, 4, 5, 6 and Theorem 2. \square

C.3 Uncertainty Quantification

Algorithm 1 together with Lemma 1 provides an efficient algorithm to compute the transmission effect of any transmission channel, given the impulse responses of the policy shock and a reduced form model. In practice, the required quantities

can only be estimated. This section therefore suggests two strategies to obtain point estimates and confidence (credible) intervals for transmission effects.

Transmission effects can be estimated in a frequentist way by simply plugging in the estimates of the relevant impulse responses and (VAR) path effects into the computational procedures described above. Because transmission effects are smooth functions of impulse responses (Theorem 3), consistency and asymptotic normality of the estimated transmission effects follow directly. Thus, point estimates of transmission effects can be obtained by using Algorithm 1 and Lemma 1 together with point estimates of the required quantities. Uncertainty can then either be quantified using the Delta method or a bootstrap approach. Whereas the former requires new cumbersome calculations for the asymptotic variance for every specific transmission effect, the latter can straightforwardly be adapted from existing bootstrap schemes for impulse responses by simply performing the point estimation of the transmission effect in every bootstrap iteration. Validity of the bootstrap also carries over from its impulse response implementation.

Alternatively to the frequentist approach, a Bayesian approach can be adopted. For each posterior draw of the parameters in equation (7), the transmission effect of a transmission channel can be computed using Algorithm 1 and Lemma 1. This provides posterior draws of the transmission effect. A point estimate can then be obtained as the posterior mean or median, and credible intervals can be formed in the usual way.

Both approaches can be used to quantify the uncertainty around point estimates of transmission effects for any number of separate transmission channels. However, when considering a full decomposition of total effects, appropriate measures of uncertainty are more complicated to construct. For example, two channels that perfectly decompose the total effect, are restricted by the fact that they have to add up to the total effect. This induces dependence between the estimates that should be accounted for when constructing uncertainty measures. By treating the two channels jointly one could construct elliptical confidence (credible) sets. How to optimally construct, or indeed communicate, them is an important direction for further research.

Appendix D Data Sources and Description

Table D.1: Data description for all variables used in Section 5.1

Variable	Description	Details/Source
Federal Funds Rate	Federal Funds Effective Rate	FRED series FEDFUNDS; taken from the replication material of McKay and Wolf (2023)
Output Gap	Measure of the output gap	ygap_hp series of Barnichon and Mesters (2020); taken from the replication material of McKay and Wolf (2023)
Inflation	Annualised log-difference of the GDP deflator	pgdp series of Ramey (2016b); taken from the replication material of McKay and Wolf (2023)
Commodity Prices	Measure of overall commodity prices	lpcom series of Ramey (2016b); taken from the replication material of McKay and Wolf (2023)
RR Instrument	Romer and Romer (2004) shock series extended by Wieland and Yang (2020)	rr_3 series of Wieland and Yang (2020); taken from the replication material of McKay and Wolf (2023)
GK Instrument	High-frequency monetary policy instrument of Gertler and Karadi (2015)	mpl_tc series of Ramey (2016b); taken from the replication material of McKay and Wolf (2023)

Table D.2: Data description for all variables used in Section 5.2

Variable	Description	Details/Source
Government Defense News Shocks	Government defense spending news shocks as a percent of real potential GDP	news series divided by pgdp and rgdp_pott6 series of Ramey and Zubairy (2018) replication material, where pdgp is the GDP deflator and rgdp_pott6 is a measure of real potential GDP based on a sixth-order polynomial
Government Defense Spending	Real government defense spending as percent of real potential GDP	See Appendix D.1
Government Spending	Real government spending as a percent of real potential GDP	ngov series divided by pgdp and rgdp_pott6 series of Ramey and Zubairy (2018) replication material, where pdgp is the GDP deflator and rgdp_pott6 is a measure of real potential GDP based on a sixth-order polynomial
GDP	Real GDP as a percent of real potential GDP	rgdp series divided by rgdp_pott6 series of Ramey and Zubairy (2018) replication material, where rgdp_pott6 is a measure of real potential GDP based on a sixth-order polynomial

D.1 Construction of Historical Government Defense Spending

In Section 5.2 we define the anticipation channel as the effect of a news shock not going through government defense spending up to horizon H . Thus, to estimate such a channel, observed government defense spending is required. Official FRED data (series A997RC1A027NBEA) is only available from 1947Q1 onwards; however all remaining data is available from 1890Q1 onwards. Thus, to fully exploit the long sample, the FRED series needs to be extended back in time. In this section we explain our methodology.

To extend the official FRED series back in time, we rely on OWID⁹ data on "Military expenditure as a share of GDP" going back to 1827. However, OWID data is at annual frequency, implying two problems. First, the series is as a share of GDP and thus must first be converted into levels. Second, all remaining data is at quarterly frequency, implying that the military spending series needs to be interpolated to quarterly frequency.

To transform the OWID series into levels, we aggregate the *ngdp* series of Ramey and Zubairy (2018) to yearly frequency and multiply this yearly nominal GDP measure with the OWID series, resulting in an approximate series of military spending in levels; however, still at annual frequency. The interpolation of this annual series to a quarterly series is then split into two parts. First, we calculate the share of annual total government spending falling into each quarter of a year (we rely on the series *ngov* of Ramey and Zubairy, 2018). Second, we multiply the quarterly shares by the yearly military spending series to obtain an interpolated quarterly military spending series. Under the assumption that the total government spending shares are approximately equal to the true shares of military spending, this interpolation method should approximate quarterly military spending well.

We check the quality of the interpolated series by comparing it to the official FRED data from 1947Q1 onwards. In levels, the two series have a correlation coefficient of 0.99 and the quarterly shares calculated using FRED data have a 0.82 correlation coefficient with the shares used to interpolate the military spending series. However, in differences, the FRED series and the interpolated series have a correlation coefficient of 0.4. Thus, some mismatch might exist. Since we only aim to demonstrate the proposed methodology, we leave robustness checks with respect to changes in the construction of the quarterly series for future research.

⁹Our World in Data (based on COW & SIPRI 2018) – processed by Our World in Data, <https://ourworldindata.org/grapher/military-expenditure-as-a-share-of-gdp-long?time=earliest..2016> accessed on February 9, 2024 at 14:30